INTERNATIONAL JOURNAL FOR NUMERICAL METHODS IN FLUIDS
Int. J. Numer. Meth. Fluids 2003; **42**:399–437 (DOI: 10.1002/fld.520)

Analysis of the local truncation error in the pressure-free projection method for incompressible flows: a new accurate expression of the intermediate boundary conditions

P. Iannelli[†] and F. M. Denaro[*,‡]

Dipartimento di Ingegneria Aerospaziale e Meccanica, Seconda Universita' degli Studi di Napoli, Italia

SUMMARY

The numerical integration of the Navier–Stokes equations for incompressible flows demands efficient and accurate solution algorithms for pressure–velocity splitting. Such decoupling was traditionally performed by adopting the Fractional Time-Step Method that is based on a formal separation between convective–diffusive momentum terms from the pressure gradient term. This idea is strictly related to the fundamental theorem on the Helmholtz–Hodge orthogonal decomposition of a vector field in a finite domain, from which the name projection methods originates. The aim of this paper is to provide an original evaluation of the local truncation error (LTE) for analysing the actual accuracy achieved by solving the de-coupled system. The LTE sources are formally subdivided in two categories: errors intrinsically due to the splitting of the original system and errors due to the assignment of the boundary conditions. The main goal of the present paper consists in both providing the LTE analysis and proposing a remedy for the inaccuracy of some types of intermediate boundary conditions associated with the prediction equation. Such evaluations will be directly performed in the physical space for both the time continuous formulation and the finite volume discretization along with the discrete Adams–Bashforth/Crank–Nicolson time integration. A new proposal for a boundary condition expression, congruent with the discrete prediction equation is herein derived, fulfilling the goal of accomplishing the closure of the problem with fully second order accuracy. In our knowledge, this procedure is new in the literature and can be easily implemented for confined flows. The LTE is clearly highlighted and many computations demonstrate that our proposal is efficient and accurate and the goal of adopting the pressure-free method in a finite domain with fully second order accuracy is reached. Copyright © 2003 John Wiley & Sons, Ltd.

KEY WORDS: fractional time-step method for incompressible flows; intermediate boundary conditions; local truncation error; Adams–Bashforth scheme; Crank–Nicolson scheme; finite volume approximation

1. INTRODUCTION

The numerical solution of the Navier–Stokes (NS) equations for isothermal, incompressible flows deals with the difficulty arising from the specific velocity–pressure coupling. In fact,

* Correspondence to: F. M. Denaro, Dipartimento di Ingegneria Aerospaziale, Seconda Universita degli Studi di Napoli, via Roma 29, 81031 Aversa (CE), Italy.
† Present Address: Centro Italiano Ricerche Aerospaziali, Capua, Italia.
‡ E-mail: denaro@unina.it

Received 1 February 2002
Accepted 19 January 2003

owing to the continuity constraint, the pressure characterizes itself only as a Lagrange multiplier, not a thermodynamic state variable. Hence, heavy computational procedures are needed for solving the resultant Stokes-like system. In order to simplify such procedures, the pressure–velocity de-coupling is often obtained by adopting a fractional time-step method (FTSM), which is based, in a specific formulation suitable for the NS equations, on a formal decomposition of the momentum equation. Specifically, the separation between the convective–diffusive terms (contributing to compute an intermediate non-solenoidal velocity field, say $\mathbf{v}^*$) and the pressure gradient term (afterwards contributing to compute a corrective pure gradient field, say $\mathbf{v}'$) is performed. This idea is strictly related to the Helmholtz–Hodge theorem on the orthogonal decomposition of a vector field in a finite domain (e.g. see References [1–5]) from which the name *projection method* originates. Thus, a prediction and a projection procedure are the sequential steps of the FTSM.

Historically, the intermediate field $\mathbf{v}^*$ is defined into the time-discretized prediction equations (e.g. see References [2, 6–10]) therefore, its meaning is strongly dependent on the adopted time integration scheme. Actually, one of the major debates still concerning the accuracy analysis of the FTSM, is based on the different meanings that $\mathbf{v}^*$ assumes in the discrete or in the continuous case, respectively. In the first case, $\mathbf{v}^*$ is only a mathematical position used for an intermediate variable while in the second case, it must be assumed to be a time continuous regular solution of a proper partial differential equation. Thus, despite of the fact that proofs of convergence for the discrete FTSM were reported in Reference [4] since 1969, various analyses on the accuracy of different methods have vivified the literature (e.g. see References [8–21]), also within conflicting argumentations. However, some of the papers that have appeared in the last few years provide a clearer explanation on the nature of the FTSM errors, assessing the actual accuracy for some types of fractional methods (among others see References [11–19]).

It is known that the original first order accurate Chorin's method causes a numerical boundary layer generated by a mismatch in the boundary conditions for $\mathbf{v}^*$ from the global error terms. Indeed, the FTSM never satisfies both normal and tangential velocity assignments on the boundaries [11–21]. The strategy of resetting, after each time step, the tangential component to its correct physical value, remains a poorly accurate procedure and can reduce the smoothness of the velocity field [17, 21]. An improvement of the Chorin's method is the *pressure-free projection method* wherein the equation for $\mathbf{v}^*$ is obtained by performing the semi-implicit multi-step Adams–Bashforth/Crank–Nicolson (in the following indicated as AB/CN) time integration of the momentum equation and by disregarding the time integral of the pressure term, thereafter. If such a method is adopted, then the velocity remains second order accurate [12], regardless of the first order accurate pressure computation. However, owing to the boundary conditions mismatch, the numerical boundary layer can still appear. As the FTSM is often practically implemented by means of such integration and the actual accuracy, which is achieved by solving the de-coupled system, is not exclusively dependent on that of each step, only the *pressure-free* projection method will be analysed in this paper. Though possible, no extension of it to other methods like the *incremental pressure* ones was considered.

Generally, any space–time discretized equation is not exactly satisfied by the true solution of the partial differential counterpart and the discrepancy consists of the so-called *local truncation error* (LTE). Thus, the accuracy of the scheme is defined by the rate at which the LTE goes to zero as the integration parameters vanish. In a single time step, the *discretization error* (i.e. the difference between the true and the numerical solution) is expressed by the LTE

multiplied by the time step [22]. In this paper, attention is devoted to the evaluation of the *splitting error*, i.e. the error introduced by the FTSM, which stands for the counterpart of the discretization error. Thus, the *splitting error* expression is first determined then the LTE associated to the FTSM is straightforwardly obtained by simply dividing it by the time step. From the LTE analysis one can subdivide the error sources in two categories:

(a) Errors intrinsically due to the splitting of the original system;
(b) Errors due to the intermediate boundary condition assignment.

The main goal of the present paper is to provide an insight into the analysis of the above points by evaluating the LTE and to propose a procedure for improving the accuracy of the boundary conditions associated to the prediction equation. Such evaluations will be directly performed in the physical space while the different meanings of the solution $\mathbf{v}^*$ will be highlighted. In particular: (1) an *ideal* exact continuous approach, (2) a continuous decoupled formulation, (3) the discrete AB/CN integration, are addressed. The introduction of the analysis for the continuous case is motivated by the fact that, in order to close the AB/CN discretized prediction equation, a similar methodology was proposed in Reference [6], based on Taylor series, for deriving intermediate boundary conditions. By doing so, it will be shown why that specific partial differential equation for $\mathbf{v}^*$ is not consistent with the AB/CN discretization whilst, the proper approach is shown to be towards the so-called *gauge equation* [11, 14, 21]. In this framework, by assuming that the solution remains regular over a given space–time interval (e.g. see the theorem on regularity in Reference [15]), the resulting expressions of the *splitting error* vectors are addressed. This way it is shown both the consistency of the AB/CN scheme towards the gauge equation and its de-coupling resulting from the specific time extrapolation applied on the convective term. Although the spatially continuous analysis of the pressure-free projection method has already been published, an original contribution of this paper consists of the LTE evaluation for the discrete formulations, which highlights the differences with the continuous counterparts. In particular, such analyses can be adopted for expressing the errors in physical space rather than in the transformed space, as it can be done with the normal mode analysis.

The second order accuracy of the discretized FTSM is maintained all the way up to the boundary of a finite computational domain, if *correct* boundary conditions (the description of what *correct* stands for is clearly illustrated in Section 5) are assigned during the prediction step. In fact, even if $\mathbf{v}^*$ is only a position for the updated discrete velocity, accurate intermediate boundary conditions are required owing to the parabolic character of the semi-implicit AB/CN prediction equation. Thus, the actual accuracy of the FTSM depends on the congruence between such a numerical scheme and the approximate boundary conditions since the projection step allows us only the imposition of one boundary condition.[§] In order to evaluate separately from the general accuracy of the FTSM, the LTE analysis of errors like (b) is performed with non-homogeneous Dirichlet boundary conditions. Then, a new proposal is herein derived consisting of a boundary condition expression fulfilling the goal of congruence while accomplishing the closure of the problem with full accuracy when associated with the

[§]It can be shown that the orthogonal decomposition admits a unique solution in case of either tangential condition or normal condition assignments.

AB/CN prediction equation. In our knowledge, this procedure is new in the literature and can be easily implemented for confined flows.

After the theory, numerical results are obtained by exploiting a second order finite volume (FV) discretization, over two finite domains with both periodic and Dirichlet boundary conditions. The accuracy study is based on the exact 2-D solution representing periodic vortex decay into the whole real space (the Taylor solution, dated 1923, e.g. see Reference [6]). When considering Dirichlet boundary conditions, two different computational domains, with boundary locations having both a vanishing and non-vanishing normal component of the pressure gradient, were adopted. This way, one analyses the cases of both orthogonal and non-orthogonal vector decompositions. In fact, if the boundary layer mode is orthogonal to the space of divergence-free vector fields, although created by inconsistent boundary conditions, the projected velocity field does not contain such errors. Therefore, in order to force the error to enter into the solution and assess the actual accuracy a proper domain in which the decomposition is not orthogonal will be considered.

By summarizing the results of this study, the numerical accuracy analysis, performed in the L_∞ norm (supposed the velocity to be a strong solution of the NS equations), is two-fold: by taking constant either the mesh size or the Courant number (CFL). In the first case, a description of a possible erroneous interpretation of the results discussed in Reference [8] is given; this is based on the consideration that the convergence analysis of the discretization error versus the time step can be misleading. It can be shown that, in a single time step, the actual slope of the discretization error curve is provided by the LTE magnitude order, multiplied by the time step (e.g. References [15, 22]). It is clearly shown why, by taking constant the mesh size, one verifies a third order slope only for high time step Δt, then a transition to monotonic first order slope caused by the $O(\Delta t h^2)$ term in the splitting error. This is what one should expect for the fully discretized FTSM as correct behaviour of the convergence error rate in the L_∞ norm. Conversely, by taking the CFL constant, the slope is monotonically third order for second order spatial discretization. The error of type (b) is clearly highlighted and many computations demonstrate that our proposal is efficient and accurate and the goal of adopting the *pressure-free* method based on AB/CN scheme with fully second order accuracy is reached.

2. THE PRESSURE-FREE PROJECTION METHOD FOR CONTINUOUS OPERATORS

Consider, in a finite domain Ω the Navier–Stokes equations for isothermal, incompressible, Newtonian, viscous flows, written in non–dimensional form

$$\underline{\nabla} \cdot \mathbf{v} \equiv D = 0 \tag{1}$$

$$\frac{\partial \mathbf{v}}{\partial t} + \underline{\nabla} \cdot (\mathbf{v}\mathbf{v}) + \underline{\nabla} p' = \underline{\nabla} \cdot \left(\frac{1}{Re} \underline{\nabla} \mathbf{v} \right) \tag{2}$$

having posed $p' = p/\rho_0 U_r^2$ and $Re = U_r L_r / \nu$ the Reynolds number. The problem consists in finding the vector fields $\mathbf{v}$ and $\underline{\nabla} p'$ satisfying (1–2) in $\Omega' = \Omega \times (t_0, t)$ for given initial $\mathbf{v}(t_0)$ (for the sake of brevity, dependence on the position $\mathbf{x}$ is herein omitted) and boundary conditions $\mathbf{v}(\mathbf{x}, t) = \mathbf{v}_\partial(t), \mathbf{x} \in \partial\Omega$, assigned along the frontier ∂.

Numerical solutions of the equations system (1), (2) require heavy computational efforts caused by the velocity–pressure coupling as the pressure is a Lagrangian multiplier, not a thermodynamic state variable. The splitting methodology, specifically devoted to the Navier–Stokes equations, which is here illustrated, is based on the Helmholtz–Hodge orthogonal decomposition theorem in a finite domain [5]. Since the original discrete Chorin's method [2] is easily deducible and elsewhere analysed (e.g. Reference [18]), no analysis of it is herein considered but the *pressure-free projection* method is focused in the following.

Let us define, in the interval (t_0, t), both the local acceleration $\partial_t \mathbf{v} =: \mathbf{a}(t)$ and the vector field $\mathbf{R}[\mathbf{v}(t)]$ such that the momentum equation (2) can be recast as

$$\mathbf{R} := -\underline{\nabla} \cdot (\mathbf{v}\mathbf{v}) + \underline{\nabla} \cdot \left(\frac{1}{Re} \underline{\nabla} \mathbf{v} \right) = \mathbf{a} + \underline{\nabla} p' =: \mathbf{a}^* \tag{3}$$

Let us suppose $\mathbf{a}^*$ to be the time derivative of a continuous vector field $\mathbf{v}^*$ (as well as, in Equation (3) $\mathbf{a}$ is the time derivative of $\mathbf{v}$) i.e. $\partial_t \mathbf{v}^* =: \mathbf{a}^*(t)$; of course, $\mathbf{v}^*(t)$ and $\mathbf{v}(t)$ are solutions of two different partial differential equations. The first question is addressed as: *in order for the solution* $\mathbf{v}^*(t)$ *to be obtained by solving a de-coupled system, in which way should Equation* (3) *be approximated?*

In fact, given the initial condition according to $\mathbf{v}^*(t_0) = \mathbf{v}(t_0)$ (i.e. such that $\underline{\nabla} \cdot \mathbf{v}^*(t_0) = 0$ is fulfilled), from time integration of Equation (3), one has

$$\mathbf{v}^*(t) = \mathbf{v}(t) + \int_{t_0}^{t} \underline{\nabla} p' \, \mathrm{d}\tau = \mathbf{v}(t_0) + \int_{t_0}^{t} \mathbf{R} \, \mathrm{d}\tau \;\Rightarrow\; \mathbf{v}^*(t) = \mathbf{v}(t_0) + (t - t_0)\langle \mathbf{R} \rangle(t) \tag{4}$$

having indicated with the symbol $\langle \bullet \rangle(t)$ an averaged function obtained by performing the time integral in the interval (t_0, t); thus, in an *ideal* case, $\mathbf{v}^*_{\mathrm{id}}(t)$ should be solution of the partial differential equation

$$\frac{\partial \mathbf{v}^*_{\mathrm{id}}}{\partial t} = \mathbf{R}[\mathbf{v}(t)] \tag{5}$$

Roughly speaking, the intermediate field $\mathbf{v}^*_{\mathrm{id}}(t)$ is related to the function $\mathbf{R}[\mathbf{v}(t)]$ (that still depends on pressure terms), therefore Equation (5) remains coupled with the solution of the continuity equation. This coupling requires a nested iterative solver procedure (similarly to the Uzawa method) and a heavy computational effort. In the spirit of the splitting methodology, one looks for some approximations allowing us to obtain an equation for determining $\mathbf{v}^*$, independently from the fulfilment of constraint (1). Thus, in order to clarify what is the meaning of the intermediate velocity, the focus point to be discussed is the way in which the vector $\mathbf{R}$ can be de-coupled from the pressure gradient.

The main approximation of the FTSM, from which several methods follow, is introduced at this point; the time evolution of $\mathbf{R}$ in the interval (t_0, t), is approximated by that of a vector, say $\mathbf{R}^*(t)$, no longer depending on the pressure gradient. Accordingly, Equation (5) is substituted¶ by $\partial_t \mathbf{v}^* = \mathbf{R}^*$, that is a partial differential equation governing the evolution

¶From now on, the subscript id will no longer be adopted because the vector $\mathbf{v}^*$ satisfies an approximate momentum equation.

of $\mathbf{v}^*$, obtained by disregarding the time contribution of the pressure gradient in $\langle \mathbf{R} \rangle(t)$ (see Equation (4)).

The choice of a proper expression for $\mathbf{R}^*$ constitutes a crucial point into the discussion of the FTSM. In fact, several possibilities are allowed to us; if one considers the following approximation

$$\mathbf{R}^* := -\underline{\nabla} \cdot (\mathbf{v}^* \mathbf{v}^*) + \underline{\nabla} \cdot \left(\frac{1}{Re} \underline{\nabla} \mathbf{v}^* \right) \tag{6}$$

it can be shown that the difference $\partial_t \mathbf{v}^* - \partial_t \mathbf{v}$ cannot be expressed as a pure gradient and this splitting would lead to a velocity field that does not satisfy the Navier–Stokes equations. On the other hand, a similar expression was proposed in Reference [6] even though only for deriving, from Taylor series, the intermediate boundary conditions for closing the semi-implicit discretized prediction equation. This fact suggested that, although Equation (6) is not used in practical computations as a real splitting method, nevertheless it is worthwhile considering it in the present analysis since, at present, intermediate boundary conditions are often derived from the proposal in Reference [6].

Besides (6), one can consider also this other approximate form

$$\mathbf{R}^* := -\underline{\nabla} \cdot (\mathbf{v}\mathbf{v}) + \underline{\nabla} \cdot \left(\frac{1}{Re} \underline{\nabla} \mathbf{v}^* \right) \tag{7}$$

expressing the so-called *gauge equation* (e.g. see References [14, 21]). Observe that in a single time interval, the integration of Equation (7) exactly corresponds to that of the *gauge* equation illustrated in References [14, 21], the differences appearing only in considering more time steps; anyway, the particular form of Equation (7) implies that the time integration of the convective term is still formally coupled with the continuity constraint. Furthermore, let us observe that, given the initial condition, Equations (6) and (7) are exactly coincident at the initial time t_0 since $\mathbf{R}^*[\mathbf{v}^*(t_0)] = \mathbf{R}[\mathbf{v}(t_0)]$; this feature will be exploited in the context of the Taylor series for the LTE evaluation.

Similarly, the de-coupled system for the perturbed equation can be also expressed in the *incremental pressure* method. Such variation implies the presence of a known gradient term in $\mathbf{R}^*$ and an update equation for the pressure (e.g. see References [12, 15, 16, 19, 21]), too. Other splitting methodologies are possible; for example, the discrete unsplit system can be approximated by a sequence of block-triangular systems (e.g. inexact LU factorization [8, 20]). The sub-problem sequence for velocity and pressure is so performed: the L-step computes the intermediate velocity field while the U-step computes the velocity correction and the pressure update, respectively. Sometimes the factorization corresponds exactly to a time discretization of the projection method. Moreover, also the class of the Yoshida method, based on the regularization of the Laplace operator, can be adopted. The method is thought to be capable of accounting for the regularizing effect of the perturbing term (pseudo-compressibility scheme-like) within the inexact factorization involving a sequence of reduced problems. The *Yoshida regularization* of the Laplace operator allows an incremental formulation of the splitting to be used [20]. Herein, these fractional methodologies are not considered.

In conclusion, whatever is the choice for the approximation $\mathbf{R}^*$, the consequence is that the formal solution for the intermediate velocity is expressed by

$$\mathbf{v}^*(t) = \mathbf{v}(t_0) + (t - t_0)\langle \mathbf{R}^* \rangle(t) \tag{8}$$

Such a velocity field does not necessarily provide the correct vorticity field $\boldsymbol{\zeta}(t)$ being $\boldsymbol{\zeta}(t) = \underline{\nabla} \wedge \mathbf{v}(t) \neq \underline{\nabla} \wedge \mathbf{v}^*(t) = \boldsymbol{\zeta}(t_0) + (t - t_0)\underline{\nabla} \wedge \langle \mathbf{R}^* \rangle(t)$; the fulfilment depends on the chosen function $\mathbf{R}^*$. From now on, according to the splitting idea, $\mathbf{v}^*$ is no longer the solution of Equation (5) but is that one expressed[‖] by the *prediction equation* (8), associated to Equation (6) or (7).

As the vector $\mathbf{v}^*(t)$ does not necessarily fulfil the constraint (1), being in general $\underline{\nabla} \cdot \langle \mathbf{R}^* \rangle \neq 0$, the projection step allows us to determine a corrective vector field, say $\mathbf{v}'(t)$. It is expressed, by definition, as a pure gradient of a time-averaged scalar function $\langle \phi \rangle$ in such a way that $\mathbf{v}^*(t) - \mathbf{v}'(t) =: \tilde{\mathbf{v}}(t)$ is a divergence-free vector ($\mathbf{v}'(t_0) = \mathbf{0}$ if the initial state is chosen such that $\underline{\nabla} \cdot \mathbf{v}^*(t_0) = 0$) which approximates the exact solution $\mathbf{v}(t)$ of the original coupled system (1), (2).

In general, the *projection equation* can be so constructed: after the field $\mathbf{v}^*(t)$ is determined by means of Equation (8) with some type of expression for $\mathbf{R}^*$, the pure gradient field is obtained by fulfilling the constraint $\underline{\nabla} \cdot \mathbf{v}'(t) = \underline{\nabla} \cdot \mathbf{v}^*(t)$ and solving the elliptic equation

$$\nabla^2 \langle \phi \rangle(t) = \frac{1}{t - t_0} \underline{\nabla} \cdot \mathbf{v}^*(t) = \underline{\nabla} \cdot \langle \mathbf{R}^* \rangle(t) \tag{9}$$

that allows us the projection of the velocity field $\mathbf{v}^*$ onto the space of divergence-free vectors. In order that problem (9) is well posed, only one condition is imposed on ∂, generally the normal derivative according to $\int_{\partial\Omega} \partial_n \langle \phi \rangle \, \mathrm{d}S = \int_{\partial\Omega} \mathbf{n} \cdot \langle \mathbf{R}^* \rangle \, \mathrm{d}S$. The fulfilment of this condition accomplishes the compatibility constraint for Neumann problems, ensuring the existence and uniqueness of the solution of (9) (apart a constant value) [5]. According to the potential character of the correction field, one has

$$\mathbf{v}'(t) \equiv \int_{t_0}^{t} \underline{\nabla} \phi \, \mathrm{d}\tau = (t - t_0)\underline{\nabla} \langle \phi \rangle(t) \tag{10}$$

and the final velocity field will be expressed by

$$\tilde{\mathbf{v}}(t) = \mathbf{v}^*(t) - \mathbf{v}'(t) = \mathbf{v}(t_0) + (t - t_0)[\langle \mathbf{R}^* \rangle(t) - \underline{\nabla} \langle \phi \rangle(t)] \tag{11}$$

that is the approximation to the exact velocity $\mathbf{v}(t)$ to be analysed. The way in which these approximations are congruent to the accuracy of a chosen numerical scheme, will be the subject of the analysis in Section 4. Therein, the expressions for the LTE in the continuous and discrete form will be provided.

[‖] It is worthwhile observing that the field $\mathbf{v}^*$ is not continuous outside the time interval: for a given $t = T$, $\mathbf{v}^*(T^-)$ and $\mathbf{v}^*(T^+)$ assume a different limiting value because, between two consecutive prediction steps, the field $\mathbf{v}^*$ computed in the first one is disregarded and $\mathbf{v}^*(T) = \mathbf{v}(T)$ will be reassigned as new initial condition for the second one. Practically, the field $\mathbf{v}^*$ is an auxiliary function that exists only in each time interval and is disregarded thereafter.

3. THE PRESSURE-FREE PROJECTION METHOD FOR DISCRETE OPERATOR: THE SECOND ORDER ACCURATE ADAMS–BASHFORTH/CRANK–NICOLSON TIME INTEGRATION

Often the semi-implicit second order accurate, Adams–Bashforth scheme for the convective term $\mathbf{R}_c \equiv -\underline{\nabla}\cdot(\mathbf{vv}) = \mathbf{R} - (1/Re)\nabla^2\mathbf{v}$ and the Crank–Nicolson scheme for the diffusive term can be exploited [6, 8, 11, 17, 20, 21]. While retaining the continuous form of the spatial operators, such kind of integration is now considered. Therefore, for prescribed divergence-free velocity vectors $\mathbf{v}^n$ and $\mathbf{v}^{n-1}$, by integrating Equation (2) in the interval $(t^n, t^{n+1} = t^n + \Delta t)$, one has

$$\begin{aligned}\left(I - \frac{\Delta t}{2\,Re}\nabla^2\right)\mathbf{v}^{n+1} &= \left(I + \frac{\Delta t}{2\,Re}\nabla^2\right)\mathbf{v}^n + \frac{\Delta t}{2}(3\mathbf{R}_c^n - \mathbf{R}_c^{n-1}) \\ &\quad - \int_{t^n}^{t^{n+1}} \underline{\nabla} p' \,\mathrm{d}t + O(\Delta t^3), \quad \mathbf{x}\in\Omega \\ \mathbf{v}_\partial(t^{n+1}) &= \mathbf{v}_\partial^{n+1}, \quad \mathbf{x}\in\partial\Omega\end{aligned} \tag{12}$$

wherein superscript notation on $\mathbf{v}$ indicates the time-discrete level of the state vectors. It is worthwhile remarking how the provisional field has not yet been introduced but the AB/CN time discretization of the momentum equation is firstly performed. The velocity field $\mathbf{v}^{n+1}$ is that one which would correspond to the numerical solution of the coupled equation system (1), (2), associated with the physical boundary conditions. This should be considered the second order accurate in time solution, adopted for reference.

By eliminating from Equation (12) the integral of the pressure gradient and truncating, the discrete equation for computing the intermediate field $\mathbf{v}^{*n+1}$ is expressed by

$$\begin{aligned}\mathbf{q} := \left(I - \frac{\Delta t}{2\,Re}\nabla^2\right)\mathbf{v}^{*n+1} &= \left(I + \frac{\Delta t}{2\,Re}\nabla^2\right)\mathbf{v}^n + \frac{\Delta t}{2}(3\mathbf{R}_c^n - \mathbf{R}_c^{n-1}), \quad \mathbf{x}\in\Omega \\ \mathbf{v}^*(t^{n+1}) &= \mathbf{v}_\partial^{*n+1}, \quad \mathbf{x}\in\partial\Omega\end{aligned} \tag{13}$$

Owing to the AB time extrapolation, such an equation has the distinctiveness, of being decoupled from continuity as the divergence-free velocity vectors are known (i.e. $\mathbf{v}^{*n} = \mathbf{v}^n$ and $\mathbf{v}^{*n-1} = \mathbf{v}^{n-1}$) whereas the CN integration leads to a semi-implicit scheme in the unknown $\mathbf{v}^{*n+1}$. Actually, while in Equation (12) the boundary condition was directly expressed in terms of the physical velocity field $\mathbf{v}_\partial^{n+1}$, now this is no longer possible. The parabolic problem (13) is associated with some type of numerical boundary condition that are not explicitly known but have to be expressed as function of the known physical velocity values, as it will discussed in Section 5. Furthermore, as Equation (13) should represent the time discretization of the continuous equation $\partial_t\mathbf{v}^* = \mathbf{R}^*$, it is necessary to determine which one of expressions (6) or (7) is implicitly discretized.

According to classical procedures, one first solves problem (13) for determining $\mathbf{v}^{*n+1}$, $\forall\mathbf{x}\in\Omega$, then solves the projection step constituted by the Poisson problem:

$$\nabla^2\langle\phi\rangle^{n+1} = \frac{1}{\Delta t}\underline{\nabla}\cdot\mathbf{v}^{*n+1}, \quad \mathbf{x}\in\Omega \tag{14}_1$$

$$\mathbf{n}\cdot\underline{\nabla}\langle\phi\rangle^{n+1} = \frac{1}{\Delta t}\mathbf{n}\cdot(\mathbf{v}^{*n+1} - \mathbf{v}_\partial^{n+1}), \quad \mathbf{x}\in\partial\Omega \tag{14}_2$$

that admits a unique solution (apart from a constant), being the compatibility condition verified by the Neumann boundary conditions $(14)_2$ with the integral continuity constraint.**

Eventually, one adds to $\mathbf{v}^{*n+1}$ the corrective velocity potential $\mathbf{v}'$, expressed as the pure gradient of $\langle\phi\rangle^{n+1}$

$$\tilde{\mathbf{v}}^{n+1} = \mathbf{v}^{*n+1} - \mathbf{v}' = \mathbf{v}^{*n+1} - \Delta t \underline{\nabla}\langle\phi\rangle^{n+1}, \quad \mathbf{x} \in \Omega \tag{15}$$

As a consequence, the projection step (14) will ensure that $\tilde{\mathbf{v}}^{n+1}$ is a divergence-free field having the correct normal component of the velocity on ∂ (i.e. $\mathbf{n}\cdot\mathbf{v}_\partial^{n+1} = \mathbf{n}\cdot\tilde{\mathbf{v}}_\partial^{n+1}$) but not necessarily fulfilling also the tangential requirement (i.e. $\mathbf{t}\cdot\mathbf{v}_\partial^{n+1} = \mathbf{t}\cdot\tilde{\mathbf{v}}_\partial^{n+1} + O(\Delta t^k)$). It is worthwhile noting that, if $\mathbf{n}\cdot\mathbf{v}_\partial^{n+1} = 0$, Equation (15) is the unique orthogonal decomposition [5] of $\mathbf{v}^{*n+1}$.

Furthermore, there exists a functional relation between $\underline{\nabla}p'$ and $\underline{\nabla}\phi$, that is determined by substituting Equation (15) into the LHS of (12) so that, in order to get a consistent second order approximation of $\tilde{\mathbf{v}}^{n+1}$ to $\mathbf{v}^{n+1}$ while verifying Equation (13), the following relationship must apply:

$$\left(I - \frac{\Delta t}{2\,Re}\nabla^2\right)\underline{\nabla}\langle\phi\rangle^{n+1} = \underline{\nabla}\langle p'\rangle^{n+1} \tag{16}$$

which clarifies the role of the computed scalar function. In fact, $\underline{\nabla}\langle\phi\rangle^{n+1}$ is only a first order approximation of the pressure gradient needed in (12), the difference consisting of a pure gradient only when gradient and Laplacian operators do commute.

A further fundamental question, to be briefly addressed, arises in discerning *which partial differential equation would Equation* (13) *tend to for vanishing time step*?

First, it is easy to see that Equation (13) cannot represent the AB/CN discretization of the *ideal* case (Equation (5) discussed in Section 2) since, although the vectors $\mathbf{R}_c^n$ and $\mathbf{R}_c^{n-1}$ correctly appear in the RHS, the diffusive term in the LHS is not that one which would be required, that is $(\mathbf{v}^{*n+1} - (\Delta t/2\,Re)\nabla^2\mathbf{v}^{n+1})$. As a matter of fact, by means of the AB discretization of the diffusive term, one could obtain a congruent second order discretization of Equation (5), too. Indeed, from a discrete viewpoint, Equation (5) would be decoupled from the pressure by adopting any explicit multi-step schemes of arbitrary accuracy order (such as Adams–Bashforth type methods); unfortunately, the numerical stability constraint is not feasible. Thus, one must analyse the consistence of (13) towards some other differential equation expressed by means of either Equation (6) or (7).

With reference to (6), one can easily see that Equation (13) does not express the AB/CN integration of $\partial_t\mathbf{v}^* = \mathbf{R}^*$; this turns out as, while is $\mathbf{R}_c^n = \mathbf{R}_c^{*n}$ from the initial condition, the vector $\mathbf{R}_c^{n-1}$ instead of that $\mathbf{R}_c^{*n-1}$ is considered (owing to the discontinuous character of $\mathbf{v}^*$, $\mathbf{v}^{*n-1}$ is disregarded outside the interval (t^n, t^{n+1}) and they are different).

**This kind of boundary condition accomplishes the fact that neither pressure nor intermediate velocity values are required on the boundary, but only the knowledge of the exact normal velocity is necessary. The final result expressed by (14) consists of an equivalent Poisson problem with homogeneous Neumann boundary conditions and a modified source term, obtained when the divergence operator is defined onto the subspace of vectors with normal component on the boundary equal to the normal velocity component; this equivalence does not imply that the computed pressure field has a vanishing normal derivative on the boundary.

Conversely, with reference to Equation (7), in the limit for $\Delta t \to 0$ one sees that Equation (13) represents the proper AB/CN discretization of the *gauge equation* $\partial_t \mathbf{v}^* = \mathbf{R}_c + 1/Re\, \nabla^2 \mathbf{v}^*$.

Although the analysis of the FTSM, for spatially continuous variables, was already described in recent [11–19] papers by means of the normal mode analysis, the original contribution of the next sections is that they illustrate the expressions of the splitting errors directly in physical rather than in transformed space. Our analysis is not the goal of debating those conclusions but is that of highlighting the fundamental differences between the continuous and the semi-implicit AB/CN approaches. Furthermore, it is performed in order to introduce the reader to the evaluation of the next proposal for a boundary condition equation, which is congruent to the correct differential equation. In fact, it will be shown that numerical boundary conditions in (13) have to be deduced while fulfilling the consistence with Equation (7).

4. THE SPLITTING ERRORS IN THE SOLUTION OF NAVIER–STOKES EQUATIONS ALONG WITH CONTINUOUS AND DISCRETE OPERATORS

In a first order accurate splitting methodology one simply replaces the exact solution operators with a sequence of numerical operators whereas in developing higher order methods, it is important to evaluate the splitting error that is introduced by the factorization. Therefore, as the FTSM is based on the separation between the pressure term and the convective–diffusive terms, even if each computational step is solved at high accuracy, the global error on $\tilde{\mathbf{v}}$ depends on some issues to be analysed.

Discretization and *local truncation errors* are the elements usually considered in numerical analysis for addressing the order of accuracy of a method. In general, the LTE is defined by the difference between a partial differential equation and its space–time discrete counterpart. The order of accuracy of a numerical scheme is defined by the rate at which the leading term of the LTE goes to zero for vanishing integration parameters. Moreover, in one time step, the *discretization error* i.e. the difference between the true and the numerical solution (which is the most adopted error measure), relates to the LTE by the time step [22] and this concept is now extended to the system splitting. Thus, the *splitting error vector* expression is determined and the LTE associated to the FTSM can be deduced in a straightforward way, by simply dividing the splitting error for the time step. This idea is formalized in Appendix A and represents the guideline of the next sub-sections. The splitting error expressions are now determined in the physical space for the cases of an analytical evaluation of $\mathbf{v}^*(t)$ based first on Equation (6) and then on (7).

4.1. The splitting error with continuous operators

Let us again consider the momentum equation (2), rewritten as

$$\frac{\partial \mathbf{v}}{\partial t} = \mathbf{R} + \mathbf{P} \equiv (L_c + L_d)\mathbf{v} + \mathbf{P} \tag{17}$$

having defined both the convective $L_c \equiv \underline{\nabla} \cdot [\mathbf{v}(\bullet)]$ and the diffusive $L_d \equiv \underline{\nabla} \cdot [\underline{\nabla}(\bullet)/Re]$ operators that act on the vector $\mathbf{v}$, while having posed $\mathbf{P} = -\underline{\nabla} p'$. Suppose that only L_d does not depend on time so that, by adopting the Taylor series about t_0, one can write (for the sake of brevity $\Delta t = t - t_0$) the exact solution of the unsplit NS system, according to the solution

operator defined in Appendix A, writes as

$$\mathbf{v}(t) = \mathbf{v}(t_0) + \Delta t \left.\frac{\partial \mathbf{v}}{\partial t}\right|_{t_0} + \left.\frac{\Delta t^2}{2}\frac{\partial^2 \mathbf{v}}{\partial t^2}\right|_{t_0} + \cdots = \sum_{j=0}^{\infty} \left.\frac{\Delta t^j}{j!}\frac{\partial^j}{\partial t^j}\right|_{t_0} \mathbf{v} \equiv \mathrm{e}^{\Delta t\, \partial/\partial t|_{t_0}} \mathbf{v}$$
$$= \mathbf{v}(t_0) + \Delta t[\langle \mathbf{R}\rangle(t) + \langle \mathbf{P}\rangle(t)] \tag{18}$$

wherein, under suitable regularity hypotheses on the initial data [15], the time derivatives can be expressed (by posing $L = L_c + L_d$, one has $\partial_t L = \partial_t L_c = -\underline{\nabla} \cdot [\partial_t \mathbf{v}(\bullet)] = -\underline{\nabla} \cdot [(\mathbf{R} + \mathbf{P})(\bullet)]$) by making successive derivatives of (17). For our goal, the second order terms are required, thus only the second derivative

$$\frac{\partial^2 \mathbf{v}}{\partial t^2} = \frac{\partial}{\partial t}(\mathbf{R} + \mathbf{P}) = \frac{\partial L_c}{\partial t}\mathbf{v} + L\frac{\partial \mathbf{v}}{\partial t} + \frac{\partial \mathbf{P}}{\partial t} = -\underline{\nabla} \cdot [(\mathbf{R} + \mathbf{P})\mathbf{v}] + L(\mathbf{R} + \mathbf{P}) + \frac{\partial \mathbf{P}}{\partial t} \tag{19}$$

is expressed. In an analogous manner, one can formally rewrite the solution (8) as

$$\mathbf{v}^*(t) = \mathbf{v}^*(t_0) + \Delta t \left.\frac{\partial \mathbf{v}^*}{\partial t}\right|_{t_0} + \left.\frac{\Delta t^2}{2}\frac{\partial^2 \mathbf{v}^*}{\partial t^2}\right|_{t_0} + \cdots = \left.\sum_{j=0}^{\infty} \frac{\Delta t^j}{j!}\frac{\partial^j}{\partial t^j}\right|_{t_0} \mathbf{v}^* \equiv \mathrm{e}^{\Delta t\, \partial/\partial t|_{t_0}} \mathbf{v}^*$$
$$= \mathbf{v}(t_0) + \Delta t \langle \mathbf{R}^*\rangle(t) \tag{20}$$

wherein, $\mathbf{v}^*(t)$ is the solution of the convection–diffusion equation $\partial_t \mathbf{v}^* = \mathbf{R}^*$ therefore, higher time derivatives in (20) must be congruently expressed first by making successive time derivations of $\mathbf{R}^*$, then by evaluating the resulting functions at the time t_0 and exploiting the initial condition.

According to the expression (48) in Appendix A, the splitting error for time continuous operators is formally defined as the difference between the exact solution (18) and the solution (11) obtained from the decoupled system, i.e. $\mathbf{e}_{fs}(t) = (\mathbf{v}(t) - \tilde{\mathbf{v}}(t))$. Two cases of possible expressions, depending on either Equation (6) or (7) respectively, will be now considered.

4.1.1. The splitting error analysis: case 1. Although expression (6) is never used as practical splitting methodology, nevertheless, a similar expression was proposed in Reference [6] specifically built for deriving second order accurate intermediate boundary conditions. Therefore, this analysis is now performed because it will be shown that those boundary conditions lead to a LTE on the boundary equivalent to the below expressed splitting error.

If one adopts expression (6) into expansion (20), then one has $\mathbf{R}^* = L^*\mathbf{v}^*$ wherein, being $L^* = L_c^* + L_d^* \equiv -\underline{\nabla} \cdot [\mathbf{v}^*(\bullet)] + L_d$, it results $\partial_t L^* = \partial_t L_c^* = -\underline{\nabla} \cdot [\partial_t \mathbf{v}^*(\bullet)] = -\underline{\nabla} \cdot [\mathbf{R}^*(\bullet)]$ along with the second derivative

$$\left.\frac{\partial^2 \mathbf{v}^*}{\partial t^2}\right|_{t_0} = \left.\frac{\partial \mathbf{R}^*}{\partial t}\right|_{t_0} = \left.\left(\frac{\partial L_c^*}{\partial t}\mathbf{v}^* + L^*\frac{\partial \mathbf{v}^*}{\partial t}\right)\right|_{t_0} = [-\underline{\nabla} \cdot (\mathbf{R}^*\mathbf{v}^*) + L^*\mathbf{R}^*]|_{t_0}$$
$$\equiv [-\underline{\nabla} \cdot (\mathbf{R}\mathbf{v}) + L\mathbf{R}]|_{t_0} \tag{21}$$

having exploited the initial condition $\mathbf{v}^*(t_0) = \mathbf{v}(t_0)$ allowing us to get $\mathbf{R}^*(t_0) = \mathbf{R}(t_0)$, $\underline{\nabla} \cdot [\mathbf{R}^*(\bullet)]|_{t_0} = \underline{\nabla} \cdot [\mathbf{R}(\bullet)]|_{t_0}$ and so on for other similar terms. Now, by using Equations (19)

and (21), one expresses the splitting error up to third order terms:

$$\begin{aligned}
\mathbf{e}_{fs}(t) &= \mathbf{v}(t) - \mathbf{v}^*(t) + \Delta t \underline{\nabla}\langle\phi\rangle(t) = \mathrm{e}^{\Delta t\partial/\partial t|_{t_0}}\mathbf{v} - \mathrm{e}^{\Delta t\partial/\partial t|_{t_0}}\mathbf{v}^* + \Delta t\underline{\nabla}\langle\phi\rangle(t) \\
&= \mathrm{e}^{\Delta t\,\partial/\partial t|_{t_0}}\Delta t(\langle\mathbf{R}\rangle - \langle\mathbf{R}^*\rangle) + \mathrm{e}^{\Delta t\,\partial/\partial t|_{t_0}}\Delta t\langle\mathbf{P}\rangle + \Delta t\underline{\nabla}\langle\phi\rangle(t) \\
&= \Delta t[\underline{\nabla}\langle\phi\rangle(t) + \langle\mathbf{P}\rangle(t)] + \Delta t[\mathbf{R}(t_0) - \mathbf{R}^*(t_0)] + \frac{\Delta t^2}{2}\left.\frac{\partial(\mathbf{R}-\mathbf{R}^*)}{\partial t}\right|_{t_0} + O(\Delta t^3) \\
&= \Delta t[\underline{\nabla}\langle\phi\rangle(t) + \langle\mathbf{P}\rangle(t)] + \frac{\Delta t^2}{2}\underbrace{\{[L(\mathbf{R}+\mathbf{P})]|_{t_0} - \underline{\nabla}\cdot[(\mathbf{R}+\mathbf{P})\mathbf{v}]|_{t_0}}_{\partial\mathbf{R}/\partial t|_{t_0}} \\
&\quad - \underbrace{[(L\mathbf{R})|_{t_0} - \underline{\nabla}\cdot(\mathbf{R}\mathbf{v})|_{t_0}]\}}_{\partial\mathbf{R}^*/\partial t|_{t_0}} + O(\Delta t^3) \\
&= \Delta t[\underline{\nabla}\langle\phi\rangle(t) + \langle\mathbf{P}\rangle(t)] + \frac{\Delta t^2}{2}\{L\mathbf{P} - \underline{\nabla}\cdot(\mathbf{P}\mathbf{v})\}|_{t_0} + O(\Delta t^3) \equiv \Delta t(\mathrm{LTE})
\end{aligned} \tag{22}$$

Consider now the L_∞ norm on the error; it follows $\|\mathbf{e}_{fs}\|_\infty = \Delta t\|\mathrm{LTE}\|_\infty$ that is the equivalent of the relation between the discretization and the local truncation error existing, for a linear scheme (e.g. see: Reference [22]), in one time step. Therefore, from examination of the leading term of (22) one can deduce $\|\mathrm{LTE}\|_\infty = (\|\underline{\nabla}[\langle\phi\rangle(t) - \langle p'\rangle(t)] + \Delta t(\cdots)\|_\infty)$ and, for the projection method to be consistent, it must result $\underline{\nabla}[\langle\phi\rangle(t) - \langle p'\rangle(t)] = O(\Delta t)$, at least. As a result of the adoption of Equation (6) for $\mathbf{R}^*$, even if one computed the exact pressure gradient, nevertheless the LTE would remain first order of magnitude, regardless of the accuracy in the solution of each single step.

4.1.2. The splitting error analysis: case 2. If one adopts Equation (7) into expansion (20) then one has $\mathbf{R}^* = L_\mathrm{c}\mathbf{v} + L_\mathrm{d}\mathbf{v}^*$ and the second derivative can be expressed as

$$\begin{aligned}
\left.\frac{\partial^2\mathbf{v}^*}{\partial t^2}\right|_{t_0} &= \left.\frac{\partial\mathbf{R}^*}{\partial t}\right|_{t_0} = \{-\underline{\nabla}\cdot[(\mathbf{R}+\mathbf{P})\mathbf{v}] + L_\mathrm{c}(\mathbf{R}+\mathbf{P}) + L_\mathrm{d}\mathbf{R}^*\}|_{t_0} \\
&\equiv \{-\underline{\nabla}\cdot[(\mathbf{R}+\mathbf{P})\mathbf{v}] + L_\mathrm{c}\mathbf{P} + L\mathbf{R}\}|_{t_0}
\end{aligned} \tag{23}$$

According to that performed in Equation (22), one has

$$\begin{aligned}
\mathbf{e}_{fs}(t) &= \mathbf{v}(t) - \mathbf{v}^*(t) + \Delta t\underline{\nabla}\langle\phi\rangle(t) \\
&= \Delta t[\underline{\nabla}\langle\phi\rangle(t) + \langle\mathbf{P}\rangle(t)] + \Delta t[\mathbf{R}(t_0) - \mathbf{R}^*(t_0)] + \frac{\Delta t^2}{2}\left.\frac{\partial}{\partial t}\right|_{t_0}(\mathbf{R}-\mathbf{R}^*) + O(\Delta t^3) \\
&= \Delta t[\underline{\nabla}\langle\phi\rangle(t) + \langle\mathbf{P}\rangle(t)] + \frac{\Delta t^2}{2}\underbrace{\{[L(\mathbf{R}+\mathbf{P})]|_{t_0} - \underline{\nabla}\cdot[(\mathbf{R}+\mathbf{P})\mathbf{v}]|_{t_0}}_{\partial\mathbf{R}/\partial t}
\end{aligned}$$

$$\underbrace{-(L_c\mathbf{P})|_{t_0} - (L\mathbf{R})|_{t_0} + \underline{\nabla}\cdot[(\mathbf{R}+\mathbf{P})\mathbf{v}]|_{t_0}\}}_{\partial\mathbf{R}^*/\partial t} + O(\Delta t^3)$$

$$= \Delta t[\underline{\nabla}\langle\phi\rangle(t) - \underline{\nabla}\langle p'\rangle(t)] - \frac{\Delta t^2}{2\,Re}\nabla^2\underline{\nabla}p'\Big|_{t_0} + O(\Delta t^3)$$

$$= \Delta t\underline{\nabla}\langle\phi\rangle(t) - \Delta t\left(I + \frac{\Delta t}{2\,Re}\nabla^2\right)\underline{\nabla}\langle p'\rangle(t) + O(\Delta t^3) \equiv \Delta t(\mathrm{LTE}) \tag{24}$$

From examination of expression (24) one gets some important conclusions; this time the LTE has no longer a first order magnitude since, by means of Equations (8) and (18) it is $\mathbf{v}(t) - \mathbf{v}^*(t) = \int_{t_0}^{t}(\mathbf{R} - \mathbf{R}^*)\,\mathrm{d}\tau - \Delta t\underline{\nabla}\langle p'\rangle(t)$ and by introducing the velocity correction $\mathbf{v}'$ one has that the relation $\Delta t\underline{\nabla}\langle p'\rangle(t) = [I - \frac{1}{Re}\nabla^2\int_{t_0}^{t}(\bullet)\,\mathrm{d}\tau]\mathbf{v}' = \mathbf{v}'(t) - \frac{\Delta t}{2\,Re}\nabla^2[\mathbf{v}'(t) + \underbrace{\mathbf{v}'(t_0)}_{=0}] + O(\Delta t^3)$ applies. Thus, the splitting error (24) is expressed as

$$\mathbf{e}_{fs}(t) = \Delta t\left[I - \left(I + \frac{\Delta t}{2\,Re}\nabla^2\right)\left(I - \frac{\Delta t}{2\,Re}\nabla^2\right)\right]\underline{\nabla}\langle\phi\rangle(t) + O(\Delta t^3)$$

$$= O(\Delta t^3) = \Delta t(\mathrm{LTE}) \tag{25}$$

thus, with regard to the velocity, this method proves to be second order accurate. Such a result does not require the commutation property between Laplacian and gradient operators and is not unexpected [14, 21] because, the gauge equation expressed by (7) is still coupled to the pressure field and the method is not a fractional one. In the context of the continuous formulation, the problem of the pressure de-coupling is still unresolved and the next section explains the difference arising from the time-discretized counterpart.

4.2. The splitting error with the AB/CN time integration and continuous space operators

It was observed in Section 3 that the use of the AB/CN time integration allows us the decoupling of the prediction equation (13) from the pressure field. This feature highlights the different meanings of the velocity $\mathbf{v}^*$ in case of the continuous differential gauge equation (where it remains coupled to the pressure) and that of the AB/CN time discretization. Actually, the obtained decoupling is a real advantage only if a third order splitting error is ensured.

Let us now analyse the splitting error for time-discretized operators, which is formally defined as the difference between the exact solution (18) and the solution (15), i.e. $\mathbf{e}_{fs}^{n+1} = (\mathbf{v}^{n+1} - \tilde{\mathbf{v}}^{n+1})$. In this case, the error $\mathbf{e}_{fs}^{n+1}$ is expressed, up to third order terms, according to

$$\mathbf{e}_{fs}^{n+1} = \mathbf{v}^{n+1} - (\mathbf{v}^{*n+1} - \mathbf{v}') = \mathrm{e}^{\Delta t\,\partial/\partial t|^n}\mathbf{v} - \left(I - \frac{\Delta t}{2\,Re}\nabla^2\right)^{-1}\mathbf{q} + \mathbf{v}'$$

$$= \mathbf{v}^n + \Delta t\left.\frac{\partial\mathbf{v}}{\partial t}\right|^n + \frac{\Delta t^2}{2}\left.\frac{\partial^2\mathbf{v}}{\partial t^2}\right|^n - \left(I + \frac{\Delta t}{2\,Re}\nabla^2 + \frac{\Delta t^2}{4\,Re^2}\nabla^2\nabla^2\right)\mathbf{q} + \mathbf{v}' + O(\Delta t^3)$$

$$= \mathbf{v}^n + \Delta t(\mathbf{R}^n + \mathbf{P}^n) - \frac{\Delta t^2}{2}\left\{ \underline{\nabla}\cdot[(\mathbf{R}^n + \mathbf{P}^n)\mathbf{v}^n] - L^n(\mathbf{R}^n + \mathbf{P}^n) - \frac{\partial \mathbf{P}}{\partial t}\bigg|^n \right\}$$

$$- \left(I + \frac{\Delta t}{2\,Re}\nabla^2 + \frac{\Delta t^2}{4\,Re^2}\nabla^2\nabla^2\right)\mathbf{q} + \mathbf{v}' + O(\Delta t^3)$$

$$= \Delta t \underbrace{\left(\mathbf{P}^n + \frac{\Delta t}{2}\frac{\partial \mathbf{P}}{\partial t}\bigg|^n + \cdots\right)}_{\underline{\nabla}\langle p'\rangle^{n+1}} + \frac{\Delta t^2}{2\,Re}\nabla^2\mathbf{P}^n + \mathbf{v}' + O(\Delta t^3)$$

$$= \Delta t\underline{\nabla}[\langle\phi\rangle^{n+1} - \langle p'\rangle^{n+1}] - \frac{\Delta t^2}{2\,Re}\nabla^2\underline{\nabla}p'^n + O(\Delta t^3) = O(\Delta t^3) \equiv \Delta t(\mathrm{LTE}) \tag{26}$$

wherein, under suitable hypothesis (see Reference [23]), the inverse operator was expressed in a power series $(I - \Delta t/2\,Re\,\nabla^2)^{-1}\mathbf{q} = (I + \Delta t/2\,Re\,\nabla^2 + \cdots)\mathbf{q}$; furthermore, the facts that the computed field $\underline{\nabla}\langle\phi\rangle^{n+1}$ satisfies Equation (16) and that $\underline{\nabla}p'^n = \underline{\nabla}\langle p'\rangle^{n+1} + O(\Delta t)$ were also exploited. In conclusion, the LTE has second order magnitude, in contrast to what is stated in Reference [8]: *the first order accuracy in the velocities is not due to boundary conditions*, *but due to the method itself because the discrete operators* $\hat{\nabla}^2$ *and* $\underline{\hat{\nabla}}$ *do not commute* (for example in case of non-periodic boundary conditions). Conversely, by looking at Equation (26) one can conclude that the second order accuracy (for the velocity) of the pressure-free FTSM (with reference to the LTE) is always maintained, consistently to the AB/CN discretization, without requiring the commutative property of the spatial operators to be verified; such a conclusion accords for example to those reported in Reference [21].

These analyses do not pretend to invalidate some published results that, while adopting other types of analysis, similarly demonstrate second order accuracy. Our aim was rather to show the splitting errors in the physical space and to relate them to the LTE in a straightforward way for practical purposes. In particular, it can be highlighted that, by extending the expression (26) to fourth order terms, one could perform an explicit spatial discretization of $\mathbf{e}_{fs}^{n+1}$ and correct again the velocity field $\tilde{\mathbf{v}}^{n+1}$ to third order accuracy, while retaining the AB/CN integration. However, such corrections must fulfil the continuity constraint by building a specific computational step; thus, this issue requires further study and is not extended in this paper. Actually, by exploiting the results of our analysis, we focus on the aim of maintaining the global accuracy all to way up to the boundary of a finite domain when non-homogeneous Dirichlet boundary conditions are assigned. In fact, we are now able in discriminating the peculiarity of the application of the FTSM into the interior of a finite domain from the application of the expression (6) for deriving intermediate boundary conditions.

4.3. Numerical accuracy study of the splitting errors

In order to assess the conclusions of the previous analyses, some numerical experiments on the continuous and discrete formulation have been performed. Let us first assume the following 2-D exact solution of Equations (1), (2) into the whole space $[-\infty, \infty]^2$ for the Reynolds number $Re = 1$ (see for example Reference [6])

$$u(x, y, t) = -\cos x \sin y \mathrm{e}^{-2t} \tag{27}_1$$

$$v(x, y, t) = \sin x \cos y \mathrm{e}^{-2t} \tag{27}_2$$

$$p'(x, y, t) = -0.25(\cos 2x + \cos 2y)\mathrm{e}^{-4t} \tag{27}_3$$

that depicts the vortex decay, studied by Taylor in 1923. When a finite domain $\Omega_1 = [-\pi, \pi] \times [-\pi, \pi]$ is considered and the solution on its boundary $\partial\Omega_1$ is expressed as prolongation of $(27)_{1,2}$, one can consider the properties required for obtaining a unique orthogonal decomposition. Both the acceleration $\mathbf{a}$ and pressure gradient fields are graphically depicted in Figures 1(a), 1(b) at time $t = 0$ from which one sees that $\mathbf{n} \cdot \underline{\nabla} p' = 0$ is accomplished along the boundaries. However, despite of the fact that $\mathbf{n} \cdot \mathbf{a} \neq 0$ on the boundaries, in $[-\pi, \pi]^2 \times [0, \infty]$ one gets $\int_{\Omega_1} \mathbf{a} \cdot \underline{\nabla} p' \, \mathrm{d}V = \int_{\partial\Omega_1} \mathbf{n} \cdot \mathbf{a} \, p' \, \mathrm{d}S = 0$, therefore $(\mathbf{a}, \underline{\nabla} p')$ (or, equivalently, $(\mathbf{v}, \Delta t \underline{\nabla} \langle p' \rangle)$ the decomposition of the vector $\mathbf{v}^*$) expresses an orthogonal decomposition of the vector field $\mathbf{a}^*$ but not a unique one. A deeper analysis of the application of the Helmholtz–Hodge decomposition in projection methods is reported in [24].

If the boundary layer mode is orthogonal to the space of divergence-free vector fields, although created by inconsistent boundary conditions, the projected velocity field does not contain such errors and full second order accuracy on the velocity is retained all the way up to the boundary. Therefore, in order to force the error to enter into the solution and assess the actual accuracy, a second finite domain $\Omega_2 = [0, \pi] \times [0, 1]$ (represented in Figure 1 by the dotted box), in which the decomposition $(\mathbf{v}, \Delta t \underline{\nabla} \langle p' \rangle)$ is not orthogonal, will be considered in Section 5.

4.3.1. Numerical accuracy study of cases 1 and 2 along with continuous operators. The analytical expression (22) and (24) that were obtained for the splitting errors, are now numerically assessed. According to the FTSM, the approximate solution to be analysed, is now expressed as

$$\tilde{\mathbf{v}}(t) = \mathbf{v}^*(t) - \mathbf{v}'(t) = \mathbf{v}(t_0) + \Delta t \left.\frac{\partial \mathbf{v}^*}{\partial t}\right|_{t_0} + \frac{\Delta t^2}{2} \left.\frac{\partial^2 \mathbf{v}^*}{\partial t^2}\right|_{t_0} - \Delta t \underline{\nabla} \langle \phi \rangle(t) + O(\Delta t^3) \tag{28}$$

wherein the two time derivatives are analytically evaluated as combinations of the spatial derivatives of the exact solution $(27)_{1,2}$ at time t_0, according to expressions (6) or (7) for $\mathbf{R}^*$. Furthermore, in order to analyse only the influence of the second and higher order terms in the (28), $\underline{\nabla} \langle \phi \rangle(t) = \underline{\nabla} \langle p' \rangle(t)$ is assigned from $(27)_3$. The error $\mathbf{e}_{fs}(t) = (\mathbf{v}(t) - \tilde{\mathbf{v}}(t))$ has been evaluated for vanishing Δt in the L_∞ norm over the finite domain Ω_1 on a (21×21) computational grid. Since this analysis concerns with the splitting error of type (a), i.e. without confinement, only such domain, wherein the decomposition is a priori orthogonal, was herein considered. All computations have been performed for a single time step so that the order of magnitude of $\mathbf{e}_{fs}$ results Δt times that of the LTE.

Starting from case 1 ($\mathbf{R}^*$ given by Equation (6), see Section 4.1.1), the error curve is computed by exploiting Equations (28) and (20), (21), (27) while assigning $\underline{\nabla} \langle \phi \rangle = \underline{\nabla} \langle p' \rangle$. The error convergence rate is shown in Figure 2; curve 1 represents the error versus the time step in a double logarithmic scale only for the u velocity component, the error on v being the same. The curve has a second order slope, which demonstrates that, albeit the third order expansion (28) has been adopted, the error is only first order accurate in time since $\|\mathbf{e}_{fs}\|_\infty = \Delta t(\|\mathrm{LTE}\|_\infty) = \Delta t O(\Delta t) = O(\Delta t^2)$. The correctness of the analysis is also confirmed by the fact that curve 2, representing the L_∞ norm applied only on the second order terms

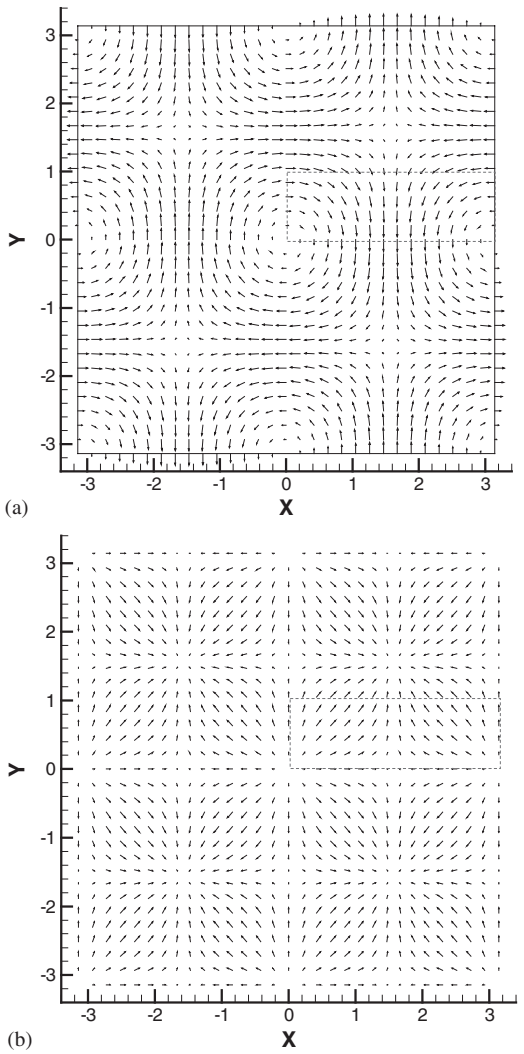

Figure 1. (a) Vector plot of the Eulerian acceleration $\mathbf{a}(\mathbf{x},0)$ in $\Omega_1=[-\pi,\pi]\times[-\pi,\pi]$. The dotted box $\Omega_2=[0,\pi]\times[0,1]$ represents a finite domain in which the decomposition is not orthogonal. (b) Vector plot of $\underline{\nabla}p'(\mathbf{x},0)$ in $\Omega_1=[-\pi,\pi]\times[-\pi,\pi]$. Note that the boundaries plot has been removed for highlighting the tangential direction of the vectors along the frontier. For a better visualisation, the vector length of Figure 1(a) has been now doubled.

$\Delta t^2/2[\mathbf{v}\nabla^2 p'+\underline{\nabla}p'\cdot(\underline{\nabla}\mathbf{v})+\mathbf{v}\cdot(\underline{\nabla}\nabla p')-\nabla^2\underline{\nabla}p'/Re]|_{t_0}$ in the error expression (22) tends, for small Δt, to become coincident to the curve 1 towards a unique second order slope, according to the analysis that predicts first order accuracy of the FTSM based on (6).

On the other hand, considering case 2 ($\mathbf{R}^*$ given by Equation (7), see Section 4.1.2), the expansion (28) must be computed with the second derivative provided by Equation (23) and $\underline{\nabla}\langle\phi\rangle(t)$ must be assigned according to Equation (16). Similarly to what was performed in

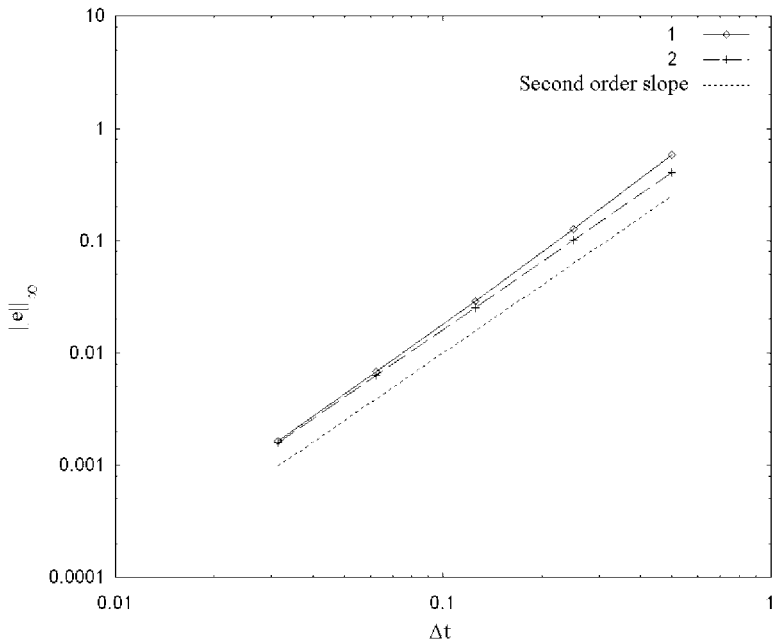

Figure 2. Analysis of the accuracy order for the FTSM with continuous operators based on Equation (6). Curve 1: L_∞ norm on $\mathbf{e}_{fs}(t)$; Curve 2: L_∞ norm of the second order terms appearing at the end of Equation (22). For small Δt, the two curves tend to become coincident.

the previous computations, the error is computed in L_∞ norm by exploiting Equations (28) and (20), (23), (27) and assigning $\underline{\nabla}\langle\phi\rangle(t) = (I + \Delta t/2\,Re\nabla^2 + \cdots)\underline{\nabla}\langle p'\rangle(t)$. The results are shown in Figure 3 versus the time step in a double logarithmic scale. In such figure, the third order slope of the error curve demonstrates that the adoption of (7) for evaluating the intermediate velocity is appropriate.

4.3.2. Numerical accuracy study based on the AB/CN time integration along with continuous space operators. Now, the error expression (26) (see Section 4.2) is verified by computing $\mathbf{v}^{*n+1}$ by means of the approximate inversion of the operator in the LHS of Equation (13)

$$\mathbf{v}^{*n+1} = \left(I - \frac{\Delta t}{2\,Re}\nabla^2\right)^{-1}\mathbf{q} = \left[I + \frac{\Delta t}{2\,Re}\nabla^2 + \left(\frac{\Delta t}{2\,Re}\nabla^2\right)^2 + \cdots\right]\mathbf{q} \tag{29}$$

that, according to the second order accuracy, can be truncated after the first three terms. This way, it is allowed us to determine $\mathbf{v}^{*n+1}$ by means of an analytical evaluation of the space derivatives of u and v given by $(22)_{1,2}$ evaluated at t^n and t^{n-1}. Hence, Equation (29) is explicit and, therefore, to compute $\mathbf{v}^{*n+1}$ in Ω is not required any approximation for the boundary conditions $\mathbf{v}_\partial^{*n+1}$. Thus, only the actual accuracy of the splitting (error type a) is evaluated. As it regards with the potential correction, according to the functional relation expressed in Equation (16), the gradient $\underline{\nabla}\langle\phi\rangle^{n+1} = (I + \Delta t/2\,Re\nabla^2 + \cdots)\underline{\nabla}\langle p'\rangle^{n+1}$ has been assigned, again by means of an analytical evaluation of the spatial derivatives of Equation

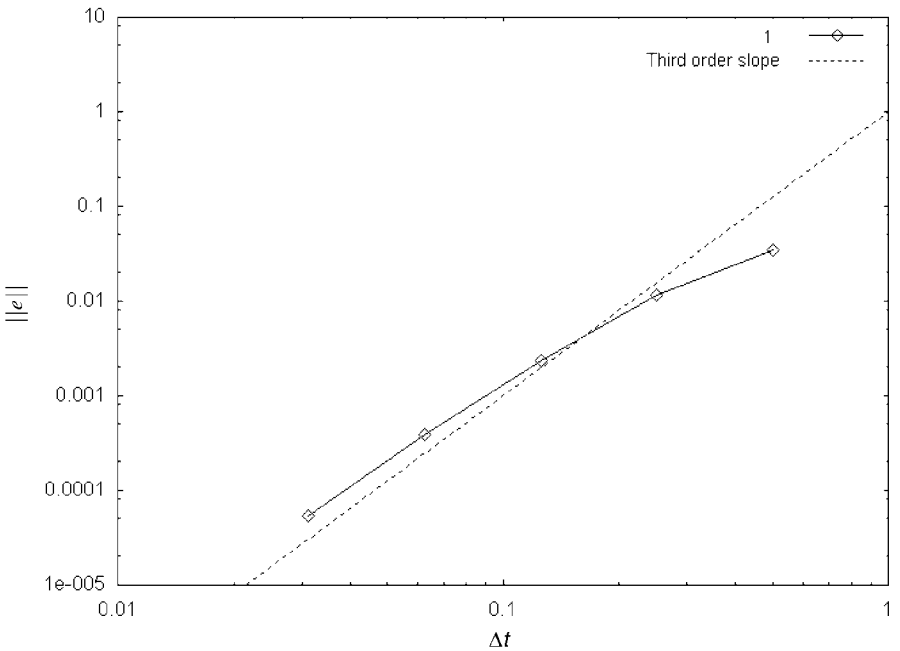

Figure 3. Analysis of the accuracy order for the FTSM with continuous operators based on Equation (7) Curve 1: L_∞ norm on the errors $\mathbf{e}_{fs}(t)$ shown versus the time step in a double logarithmic scale only for the u velocity component (the error on v being the same).

$(27)_3$. Clearly, Laplacian and gradient operators do commute in the periodical case and one obtains a pure gradient term. The error on the u velocity component is still computed for vanishing time steps in the L_∞ norms; the third order slope of curve 1 in Figure 4 clearly confirms that the velocity $\tilde{\mathbf{v}}^{n+1}$ is a third order approximation to $\mathbf{v}^{n+1}$. Of course, what is inadequate is that the field $\underline{\nabla}\langle\phi\rangle^{n+1}$ remains a first order accurate approximation of the actual pressure gradient. On the other hand, in the pressure-free methodology, one always computes only $\underline{\nabla}\langle\phi\rangle^{n+1}$ whereas the knowledge of actual pressure $\underline{\nabla}p'$ is, usually, never required.

One can draw an important conclusion: the *gauge equation* is accurate and, owing to the AB extrapolation, can be congruently decoupled from pressure. The present study indicates that, by means of the AB/CN scheme, the discretization error in the computation of the velocity is always third order in a single time step, independently from the commutation property of the gradient and Laplacian operator. In the next section, a numerical analysis for the AB/CN time integration, but associated to a second order Finite Volume discretization along with both periodical and Dirichlet boundary conditions, will be presented. This analysis is performed in order to clarify the sources of the errors of type (b) that many times has generated controversy in the published analyses.

4.3.3. Numerical accuracy study based on the AB/CN time integration along with second order finite volume space discretization. Now, a numerical accuracy study of the FTSM along with a space–time second order discretization is shown. In order to accomplish the

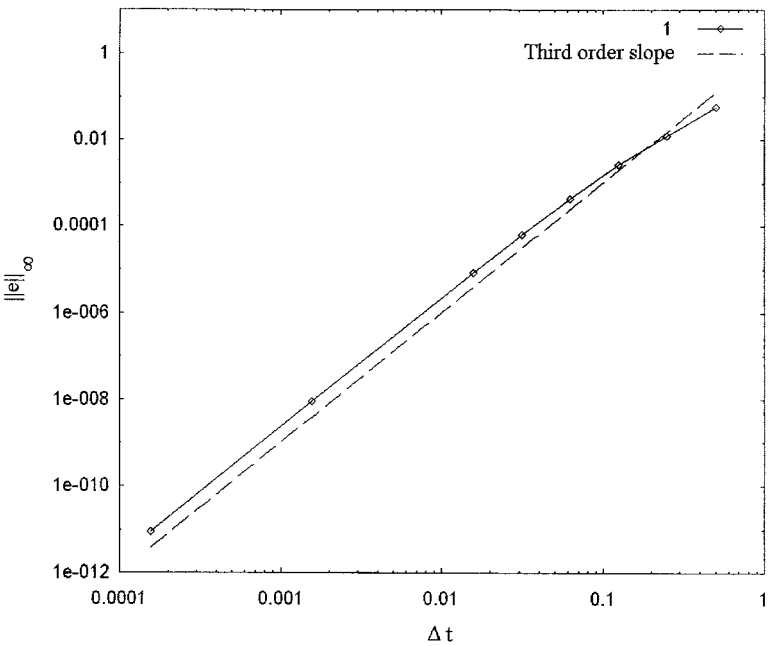

Figure 4. Analysis of the accuracy order for the FTSM based on AB/CN second order scheme (13). Curve 1: the errors, computed in the L_∞ norm in the domain Ω_1, are shown versus the time step in a double logarithmic scale only for the u velocity component (the error on v being the same).

spatial discretization, a finite volume (FV) scheme has been adopted for discretizing the operators in the integral form of Equations (1), (2) written over N control volumes.

A slight modification of the time integration procedure is performed: only the y-diffusive component has been discretized with the Crank–Nicolson scheme while the x-one has been computed within the Adams–Bashforth integration, as well as the other convective terms. This is done since such kind of discretization is a useful model for simulating 3-D confined flows. In fact, because of the thin boundary layers along the walls, the normal wall derivatives are greater in magnitude than the stream-wise ones and therefore a stretched grid, normal to the wall, is necessary. Thus, owing to stability restrictions, an implicit Crank–Nicolson integration of the diffusive terms in normal direction is considered (e.g. see Reference [25]). A further advantage is also deduced from the previous analysis because, by computing the x-diffusive component with the Adams–Bashforth scheme, the first order pressure error remains only due to the y-component of Laplacian operator and, therefore, is proportional (see Equation (16)) to the second derivative along y of the pressure gradient that in the boundary layer almost vanishes. The discretized constraint $D = 0$ is supposed to be satisfied, in an approximate projection, by the vector $\tilde{\mathbf{v}}$ only to within the local truncation error of the scheme (e.g. see Reference [26]). Hence, the NS system is rewritten according to the integral pressure-free FTSM:

Prediction step:

$$\int_{\Omega_k}\left(I-\frac{\Delta t}{2\,Re}\,\frac{\partial^2}{\partial y^2}\right)\mathbf{v}^{*n+1}\,\mathrm{d}V$$
$$=\int_{\Omega_k}\left(I+\frac{\Delta t}{2\,Re}\,\frac{\partial^2}{\partial y^2}\right)\mathbf{v}^{n}\,\mathrm{d}V$$
$$+\frac{\Delta t}{2}\int_{\Omega_k}\left[\frac{1}{Re}\left(3\frac{\partial^2\mathbf{v}^n}{\partial x^2}-\frac{\partial^2\mathbf{v}^{n-1}}{\partial x^2}\right)+3\mathbf{R}_{\mathrm{c}}^{n}-\mathbf{R}_{\mathrm{c}}^{n-1}\right]\mathrm{d}V,\quad \mathbf{x}\in\Omega$$

$$\mathbf{v}_{\partial}^{*n+1}=f(\mathbf{v}),\quad \mathbf{x}\in\partial\Omega$$

Projection step:

$$\int_{\partial\Omega_k}\mathbf{n}\cdot\underline{\nabla}\langle\phi\rangle^{n+1}\,\mathrm{d}S=\frac{1}{\Delta t}\int_{\partial\Omega_k}\mathbf{n}\cdot\mathbf{v}^{*n+1}\,\mathrm{d}S,\quad \mathbf{x}\in\Omega$$

$$\mathbf{n}\cdot\underline{\nabla}\langle\phi\rangle^{n+1}=\frac{1}{\Delta t}(\mathbf{v}^{*n+1}-\mathbf{v}_{\partial}^{n+1}),\quad \mathbf{x}\in\partial\Omega$$

Correction step:

$$\int_{\Omega_k}\tilde{\mathbf{v}}^{n+1}\,\mathrm{d}V=\int_{\Omega_k}\mathbf{v}^{*n+1}\,\mathrm{d}V-\Delta t\int_{\partial\Omega_k}\mathbf{n}\langle\phi\rangle^{n+1}\,\mathrm{d}S,\quad \mathbf{x}\in\Omega$$
$$\mathbf{v}^{n+1}=\mathbf{v}_{\partial}^{n+1},\quad \mathbf{x}\in\partial\Omega \tag{30}$$

A Cartesian uniform structured 2-D computational grid is adopted over Ω_1. If the control point (i,j) is the centre of Ω_k and the measure of Ω_k is space-independent (integrals and derivatives do commute), the second order discretization can be written according to (the notation of shift operator is introduced):

Prediction step:

$$\left(I-\frac{\Delta t}{2\,Re}\,\frac{E^{-\Delta y}-2I+E^{\Delta y}}{\Delta y^2}\right)_{i,j}\mathbf{v}^{*n+1}$$
$$=\left(I+\frac{\Delta t}{2\,Re}\,\frac{E^{-\Delta y}-2I+E^{\Delta y}}{\Delta y^2}\right)_{i,j}\mathbf{v}^{n}$$
$$+\frac{\Delta t}{2}\left[\frac{1}{Re}\left(\frac{E^{-\Delta x}-2I+E^{\Delta x}}{\Delta x^2}\right)_{i,j}(3\mathbf{v}^n-\mathbf{v}^{n-1})+(3\hat{\mathbf{R}}_{\mathrm{c}}^{n}-\hat{\mathbf{R}}_{\mathrm{c}}^{n-1})_{i,j}\right],$$
$$\mathbf{x}_{i,j}\in\Omega \tag{31}_1$$

Projection step:

$$\left[\frac{\Delta y}{\Delta x}(E^{(\Delta x/2)}-E^{-(\Delta x/2)})_{i,j}(E^{(\Delta x/2)}-E^{-(\Delta x/2)})\right.$$
$$\left.+\frac{\Delta x}{\Delta y}(E^{(\Delta y/2)}-E^{-(\Delta y/2)})_{i,j}(E^{(\Delta y/2)}-E^{-(\Delta y/2)})\right]\langle\phi\rangle^{n+1}$$
$$=\frac{\Delta y}{\Delta t}(E^{(\Delta x/2)}-E^{-(\Delta x/2)})_{i,j}\,u^{*n+1}$$
$$+\frac{\Delta x}{\Delta t}(E^{(\Delta y/2)}-E^{-(\Delta y/2)})_{i,j}v^{*n+1},\quad \mathbf{x}_{i,j}\in\Omega \tag{31}_2$$

$$(E^{\pm(\Delta x/2)})_{i,j}\left(\frac{E^{(\Delta x/2)}-E^{-(\Delta x/2)}}{\Delta x}\right)\langle\phi\rangle^{n+1}$$
$$=\frac{1}{\Delta t}(E^{\pm(\Delta x/2)})_{i,j}(u^{*n+1}-u_{\partial}^{n+1}),\quad \mathbf{x}_{i\pm\Delta x/2,j}\in\partial\Omega \tag{31}_3$$

$$(E^{\pm\Delta y/2})_{i,j}\left(\frac{E^{(\Delta y/2)}-E^{-(\Delta y/2)}}{\Delta y}\right)\langle\phi\rangle^{n+1}$$
$$=\frac{1}{\Delta t}(E^{\pm(\Delta y/2)})_{i,j}(v^{*n+1}-v_{\partial}^{n+1}),\quad \mathbf{x}_{i,j\pm\Delta y/2}\in\partial\Omega \tag{31}_4$$

Correction step:

$$\tilde{\mathbf{v}}_{i,j}^{n+1}=\mathbf{v}_{i,j}^{*n+1}-\Delta t\hat{\underline{\nabla}}\langle\phi\rangle_{i,j}^{n+1},\quad \mathbf{x}_{i,j}\in\Omega \tag{31}_5$$

where $\hat{\mathbf{R}}_c$ indicates a standard second order central discretization of the convective terms. The elliptic equation is discretized in the same velocity location by a five-point stencil. This way leads to the approximate projection method (e.g. see Reference [26]) and continuity is satisfied up to the local truncation error of the projection equation; owing to the strong coupling of the stencil, there are no spurious modes associated to the pressure solution.

It is fundamental to observe the way in which the space discretization affects the LTE as it is expected that the splitting error due to the FTSM (31) should be in the form $\mathbf{e}_{fs}^{n+1}=\Delta t(\mathrm{LTE})=\Delta tO(\Delta t^2,\Delta x^2,\Delta y^2)$. Similarly to what is done in Reference [8], a uniform grid size h has been fixed and the computations have been performed, by varying the time step, at different Courant numbers. Consequently, in order for those LTE terms proportional to $\Delta tO(h^2)$, to be smaller than those $\Delta tO(\Delta t^2)$, in a suitable range of $\Delta t>h$, a grid size $\Delta x=\Delta y=h=10^{-2}$ (629×629 points) was chosen. Nevertheless, one must carefully perform the accuracy analysis when $\Delta t<h$. In fact, as the derivatives of the (27) are of unitary order of magnitude, a leading term in the LTE remains proportional to h^2 and will produce, apparently, a monotonic first order convergence of the splitting error curve. This appearance can create some confusion in the analysis but it must be clear that the first order

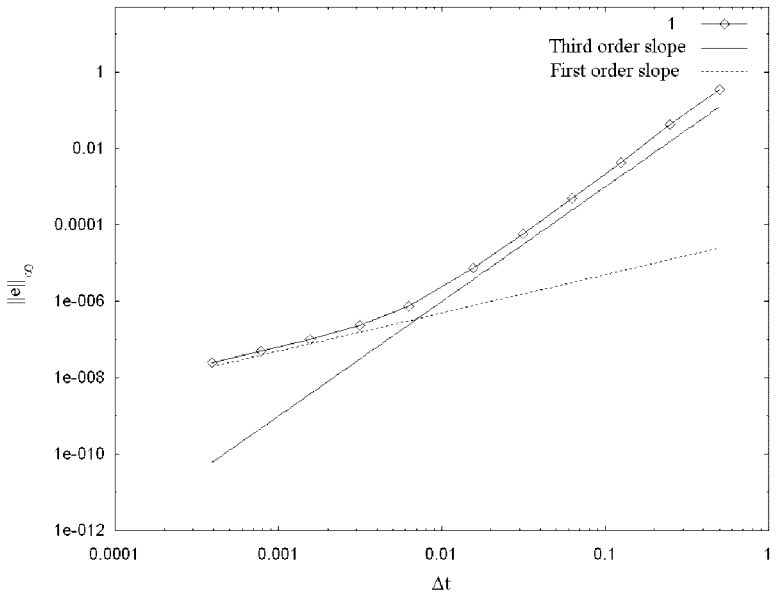

Figure 5. Analysis of the accuracy order for the FTSM based on AB/CN time integration and second order FV discretization. Curve 1: the errors, computed in the L_∞ norm in the domain Ω_1, are shown versus the time step in a double logarithmic scale only for the u velocity component (the error on v being the same).

slope appearing for small Δt is not the real accuracy of the FTSM but is only a consequence of having maintained h fixed.

In order to highlight the features of the methodology first for the case without confinement approximations, a series of computations is performed for two-periodical boundary conditions. The velocity $\mathbf{v}^{*n+1}$ is computed from $(31)_1$ by means of the Thomas algorithm and the pressure equation $(31)_2$ is solved by means of a line Gauss–Seidel solver. Furthermore, in order to assess the second order time accuracy without taking care of stability constraints, the errors have been computed in the L_∞ norm after a single time step and are reported in Figure 5 versus the time step Δt in a double logarithmic scale. The figure illustrates all the previously discussed salient features: the initial slope 3 of curve 1 confirms the second order accuracy of the pressure-free projection method but when the LTE analysis is performed for $\Delta t < h$ then the slope clearly changes from 3 up to a monotonic first order slope. This fact well accords to the fact that the discretization error becomes Δt times the leading term, proportional to h^2, in the LTE. In our knowledge, this LTE analysis of the fully discretized FTSM was not considered elsewhere.

As a matter of fact, the conclusion that the pressure-free FTSM along with the AB/CN discretization remains second order accurate (or equivalently the velocity error is $O(\Delta t^3)$ in a step) is not new in the case of periodical boundary conditions. Already in Reference [8] this result was highlighted while deducing that it is due to the fact that the discrete operators $\hat{\nabla}^2$ and $\underline{\hat{\nabla}}$ do commute when periodic boundary conditions are in effect. Conversely, in order to obtain a third order slope on the discretization error, this property does not appear from the

present analysis. Since in Reference [8] a first order slope was shown in a non-periodic case, it was therein proposed a correction that should only improve the pressure accuracy, not the velocity one. Owing to the lack in the exact knowledge of those computational conditions, an unequivocal explanation of such reported differences in the velocity errors curves (especially the reported first order slope) cannot be herein addressed. However, it is worthwhile observing that, instead of an analytical solution, the author used as comparison that one obtained on the finest grid. This kind of comparison can produce a slope of the error curve not consistent with the actual accuracy of the LTE. Furthermore, it was not considered the possible effect, produced by the constant grid size, which causes the appearance of the first order convergence.

On the other hand, in regard to the accuracy study of the *pressure-free* projection method reported in Reference [21], it is stated for the assignment of $\mathbf{v}^*$ on the frontier '*using the normal mode analysis that this is also a necessary condition for the second order accuracy*' and that '*... is surprising that projection method III* [6] *does not obtain full second order accuracy*'. In the present study, why the adoption of (6) for deriving intermediate boundary conditions would always lead to first order accurate velocity computation, was clearly explained.

5. THE LTE ANALYSIS OF THE SPACE–TIME DISCRETIZED FTSM; EFFECTS OF THE APPROXIMATE BOUNDARY CONDITION

From the analysis of the original Chorin's method, adopted along with homogeneous Dirichlet boundary conditions, it is well known the presence of a numerical boundary layer that is generated by mismatch in the boundary conditions for $\mathbf{v}^*$ from the global error terms. Then, it was shown [11–21] how the FTSM never allows us to simultaneously satisfy both normal and tangential velocity conditions on the boundary. The most adopted remedy is simply to reset, after each time step, the tangential component to its correct physical value on the boundary but it was also shown why such a procedure remains low order accurate [17] as well as it can produce a reduction in the smoothness of the solution close to the boundary.

In fact, even if $\mathbf{v}^{*n+1}$ is only a mathematical position for the updated state vector defined in Equation $(31)_1$, approximate numerical boundary conditions are someway required owing to the parabolic character of the semi-implicit prediction equation. Therefore, while the projection step $(31)_{2,3,4}$ imposes the correct normal velocity values along the boundaries, major care must be devoted to the assignment of the tangential conditions in $(31)_1$ as Equation $(31)_5$ cannot allow us further correction. According to the remark in Reference [21], the boundary condition for determining $\mathbf{v}^{*n+1}$ must be consistent to the projection step although at the time they are applied, the function $\underline{\nabla}\langle\phi\rangle^{n+1}$ is not yet known. In order to overcome the problem of approximating the pressure gradient along the boundary, a new proposal of a consistent boundary condition equation, which is based solely on the velocity field, is herein derived. This equation, when associated with the AB/CN prediction equation, accomplishes the goal of the closure of the problem with full second order accuracy. In our knowledge, this procedure is new in the literature and can be easily implemented for confined flows.

On the other hand, since many years ago [27], the determination of the correct intermediate boundary conditions is a well-known problem in factorization methods but it was often under valuated in practical computations. It is usually reputed that it is sufficient to have boundary conditions which are one order of accuracy lower than the LTE into the interior as was shown

for hyperbolic equations in Reference [28] or as it results from maximum principle for linear parabolic equations. However, practical computations found that such lower order of accuracy can lead to a large increasing of the LTE. Regardless of the rate of convergence, the errors on any grid points may be greater than required and this fact can become unacceptable in some specific kind of computations (see Section 6). The order of accuracy will be congruent to the global one in the interior, provided that *correct* boundary conditions $\mathbf{v}_{\partial}^{*n+1}$ are assigned in solving $(31)_1$: this is the LTE analysis of type (b) which was mentioned in the Introduction and is now developed. Moreover, the role of the location of the boundary is investigated; some computations with Dirichlet boundary conditions were performed also in a particular finite domain wherein the decomposition is no longer orthogonal and the pressure gradient has a non-vanishing normal component.

5.1. Taylor series-based boundary conditions

According to the proposal in Reference [6], $\mathbf{v}^*$ is supposed to be a continuous function of time and approximate boundary conditions for it were deduced by using a second order accurate Taylor expansion about the time t^n

$$\mathbf{v}^{*n+1} = \mathbf{v}^{*n} + \Delta t \left.\frac{\partial \mathbf{v}^*}{\partial t}\right|^n + O(\Delta t^2) = \mathbf{v}^n + \Delta t \left.\left(\frac{\partial \mathbf{v}}{\partial t} + \underline{\nabla} p'\right)\right|^n + O(\Delta t^2)$$

$$= \mathbf{v}^{n+1} + \Delta t \underline{\nabla}\langle\phi\rangle^n + O(\Delta t^2) \Rightarrow \mathbf{v}_{\partial}^{*n+1} = \mathbf{v}_{\partial}^{n+1} + \Delta t \underline{\nabla}\langle\phi\rangle_{\partial}^n \tag{32}$$

In this expression, the knowledge of $\underline{\nabla}\langle\phi\rangle_{\partial}^n$ is required therefore, it must be retained for this aim in each time step. However, this kind of boundary condition has some incongruent implication:

(I) Expansion (32) is not congruent to the order of the time integration (13) that is $O(\Delta t^3)$ in a single time step. It is expected that the LTE will degrade to first order[††] magnitude near the boundaries since the projection step will enforce $\partial_n \phi^{n+1} = \partial_n \phi^n = \cdots \partial_n \phi^0$ on ∂, a numerical boundary layer [11–21] is generated. This fact can deteriorate the solution into the interior, although the convergence of discrete FTSM was proved [4].

(II) Expansion (32) was derived by means of the differential equation $\partial_t \mathbf{v}^* = \mathbf{R}^*$, being $\mathbf{R}^*$ expressed by Equation (6). Thus, even if the infinite expansion (20) were adopted, the resulting expression for $\mathbf{v}_{\partial}^{*n+1}$ would not correspond to that required as consistent boundary condition for the AB/CN integration. This conclusion appears now straightforward in the light of the previous analyses: again, the problem results into the mismatch of the vector $\mathbf{v}^*$ for the discrete or continuous approach. Such mismatch is resolved by the projection step with respect to the normal component, nothing being corrected for what it regards with the tangential component.

(III) It is easy to verify that expansion (32), if truncated to the second order, can not take any advantage by adopting $\mathbf{R}^*$ expressed by Equation (7); in fact, Equations (6) and (7) are coincident at time t^n the first difference appearing from the time derivative $\partial_t \mathbf{R}^*$.

From such issues, it follows that the second order term must be retained into the expansion.

[††]In some papers, analysing Stokes flows, the resulting order of accuracy is reported as $O(\Delta t^{1/2})$ because of the adopted constant rate $\Delta t/h^2$.

5.2. *A consistent and accurate intermediate boundary condition expression and its space discretization*

An original strategy to derive an accurate expression for $\mathbf{v}_\partial^{*n+1}$ is now illustrated. The starting point of the analysis is that the vector $\mathbf{v}_\partial^{*n+1}$ must be consistent both to the AB/CN discretized equation $(31)_1$ and to the projection step $(31)_{2,3,4}$ while, at the time it must be applied, the function $\underline{\nabla}\langle\phi\rangle^{n+1}$ is not yet computed.

Consider Equation $(31)_1$ so that, whatever Ω_k is, the resulting differential equation with the space operators in continuous form, has a solution expressed according to the point-wise relation:

$$\begin{aligned}
\mathbf{v}^{*n+1} &= \left(I - \frac{\Delta t}{2\,Re}\,\frac{\partial^2}{\partial y^2}\right)^{-1}\left\{\left[I + \frac{\Delta t}{2\,Re}\left(\frac{\partial^2}{\partial y^2} + 3\,\frac{\partial^2}{\partial x^2}\right)\right]\mathbf{v}^n\right.\\
&\quad\left. + \frac{\Delta t}{2}\left(3\mathbf{R}_c^n - \mathbf{R}_c^{n-1} - \frac{1}{Re}\,\frac{\partial^2 \mathbf{v}^{n-1}}{\partial x^2}\right)\right\} = \left(I + \frac{\Delta t}{2Re}\,\frac{\partial^2}{\partial y^2} + \frac{\Delta t^2}{4Re^2}\,\frac{\partial^4}{\partial y^4} + \cdots\right)\mathbf{q}'\\
\Rightarrow \mathbf{v}_\partial^{*n+1} &= \left(I + \frac{\Delta t}{2\,Re}\,\frac{\partial^2}{\partial y^2} + \frac{\Delta t^2}{4\,Re^2}\,\frac{\partial^4}{\partial y^4}\right)\Big|_\partial \mathbf{q}' = \left\{\left(I + \frac{\Delta t}{Re}\,\frac{\partial^2}{\partial y^2} + \frac{\Delta t^2}{4\,Re^2}\,\frac{\partial^4}{\partial y^4}\right)\mathbf{v}^n\right.\\
&\quad\left. + \left(\frac{\Delta t}{2} + \frac{\Delta t^2}{4\,Re}\,\frac{\partial^2}{\partial y^2}\right)\left[\frac{1}{Re}\,\frac{\partial^2}{\partial x^2}(3\mathbf{v}^n - \mathbf{v}^{n-1}) + 3\mathbf{R}_c^n - \mathbf{R}_c^{n-1}\right]\right\}\Big|_\partial
\end{aligned} \tag{33}$$

The expression derived on the boundary was the limiting value, obtained from the interior, wherein only terms up to $O(\Delta t^2)$ will be retained into the approximate inversion. The attractive feature of the proposal is that, although the gradient of ϕ along the boundary no longer appears, the expression (33) is consistent with Equations (30), as mathematically proved in Appendix B.

The space discretization of the derivatives in Equation (33) requires a proper backward/forward stencil to take into account for the accurate evaluation of $\mathbf{v}_\partial^{*n+1}$ along the boundary. Since the asymmetry of the stencil can alter the resulting expression of the local truncation error, in order to briefly clarify this issue let us consider the linear diffusion equation $\partial_t\varphi = \partial_{xx}\varphi$. When it is discretized by means of the classical CN scheme in time and central second order discretization in space, the LTE results $O(\Delta t^2, h^2)$, according to the *modified equation*:

$$\frac{\partial\varphi}{\partial t} - \frac{\partial^2\varphi}{\partial x^2} = \left(\frac{\Delta t^2}{12}\,\frac{\partial^6\varphi}{\partial x^6} + \frac{h^2}{12}\,\frac{\partial^4\varphi}{\partial x^4} + \frac{\Delta t h^2}{24}\,\frac{\partial^6\varphi}{\partial x^6} + \cdots\right) \tag{34}$$

On the other hand, by adopting the approximate inversion (33) one has $\varphi_i^{n+1} = (1 + \Delta t\partial_{xx} + \Delta t^2/2\partial_{xxxx})_i\varphi^n$, which could be discretized with a central second order accurate formula (again, shift notation is adopted), leading to the scheme:

$$\varphi_i^{n+1} = \left[I + \Delta t\,\frac{(E^h - 2I + E^{-h})}{h^2} + \frac{\Delta t^2}{2}\,\frac{(E^{2h} - 4E^h + 6I - 4E^{-h} + E^{-2h})}{h^4}\right]\varphi_i^n \tag{35}$$

while, a backward second order formula, which is suitable to be adopted for discretizing (33) on to the boundary, leads to

$$\varphi_i^{n+1} = \left(I + \Delta t \, \frac{2I - 5E^{-h} + 4E^{-2h} - E^{-3h}}{h^2} + \frac{\Delta t^2}{2} \, \frac{3I - 14E^{-h} + 26E^{-2h} - 24E^{-3h} + 11E^{-4h} - 2E^{-5h}}{h^4} \right) \varphi_i^n \tag{36}$$

Accordingly, one gets the following LTE:

$$\frac{\partial \varphi}{\partial t} - \frac{\partial^2 \varphi}{\partial x^2} = \left(-\frac{\Delta t^2}{6} \, \frac{\partial^6 \varphi}{\partial x^6} + \frac{h^2}{12} \, \frac{\partial^4 \varphi}{\partial x^4} + \frac{\Delta t h^2}{12} \, \frac{\partial^6 \varphi}{\partial x^6} + \cdots \right) \tag{37}$$

for Equation (35) and

$$\frac{\partial \varphi}{\partial t} - \frac{\partial^2 \varphi}{\partial x^2} = \left(\frac{\Delta t^2}{6} \, \frac{\partial^6 \varphi}{\partial x^6} - \frac{11}{12} \, h^2 \, \frac{\partial^4 \varphi}{\partial x^4} - \frac{17}{12} \, \Delta t h^2 \, \frac{\partial^6 \varphi}{\partial x^6} + \cdots \right) \tag{38}$$

for (36), respectively. These expressions show that, if one performs an accuracy study for vanishing Δt but by taking a constant mesh size h, one observes a discretization error curve according to a polynomial of the type $(a\Delta t + b\Delta t^2 + c\Delta t^3 + \cdots)$ and, however, a first order slope for small Δt. The way in which the error curve tends to first order slope, will depend on the coefficients into the modified equation that are different for central or backward discretization. However, this appearance is common also for the classical CN discretization, as highlighted by Equation (34), and the discretization (36) lead to a congruent evaluation on the boundary. Considering, for example, an upper boundary at $j = JB$, one gets

$$\mathbf{v}_{i,JB}^{*n+1} = \hat{\mathbf{q}}'_{i,JB} + \frac{\Delta t}{2 Re \Delta y^2} (2I - 5E^{-\Delta y} + 4E^{-2\Delta y} - E^{-3\Delta y})_{i,JB} \hat{\mathbf{q}}' + \frac{\Delta t^2}{4 Re^2 \Delta y^4} \times (3I - 14E^{-\Delta y} + 26E^{-2\Delta y} - 24E^{-3\Delta y} + 11E^{-4\Delta y} - 2E^{-5\Delta y})_{i,JB} \mathbf{v}^n \tag{39}$$

wherein $\hat{\mathbf{q}}'$ is the RHS of $(31)_1$ for all the interior points and $\hat{\mathbf{q}}'_{i,JB}$ is that one evaluated on a backward stencil. Observe that in some cases one can suppose sufficiently correct to disregard the terms $O(\Delta t^2 / Re^2)$ and simplify (40).

5.3. *Results*

In order to assess both the general analyses and the validity of our proposal, the vortex decay problem is now resolved prescribing several combinations of the boundary conditions. First the problem is solved in Ω_1 along with Dirichlet boundary conditions assigned at $y = \pm \pi$ while retaining the periodicity at $x = \pm \pi$. Exactly the previous mesh size h and time steps have been adopted and the errors, obtained again in the L_∞ norm, are evaluated after a single time step onto the boundary points, too. In the first runs, the first order boundary condition (32) are tested since they are those proposed in Reference [6], analysed in many papers [11–21] and adopted in many simulations. In this case, the error convergence rates for u and v are reported in Figure 6 versus the time step Δt, in a double logarithmic scale. The plot shows only a second order slope before the curves tend towards the first order one for

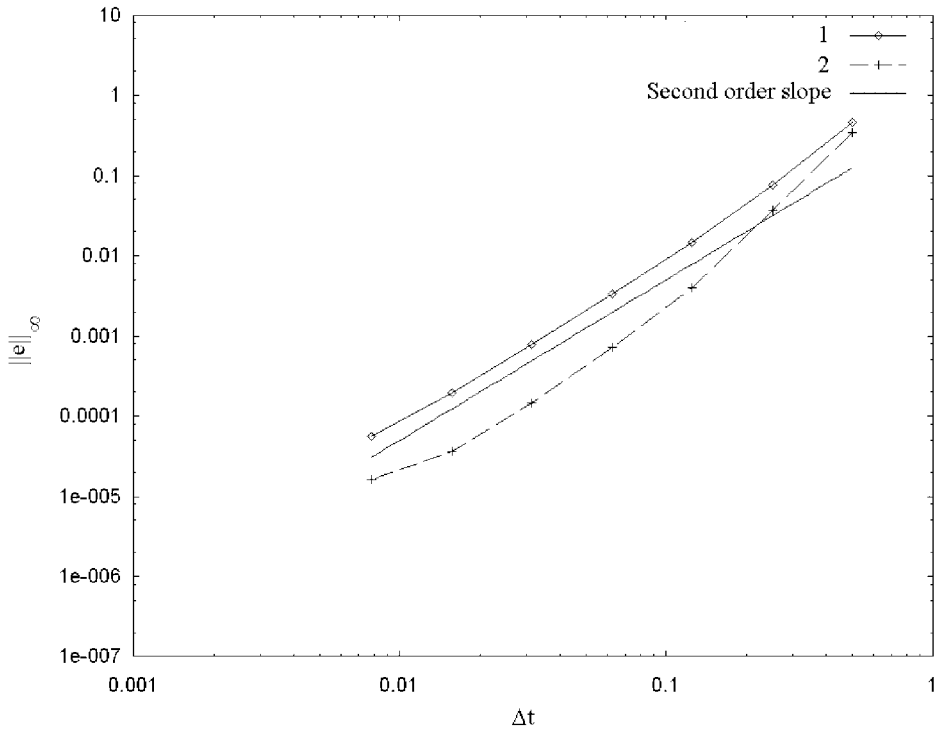

Figure 6. Analysis of the accuracy order for with the FTSM based on AB/CN time integration and second order FV discretization and Dirichlet boundary conditions [6]. The errors, computed in the L_∞, norm in the domain Ω_1, are shown versus the time step in a double logarithmic scale for both u (curve 1) and v (curve 2) velocity components.

$\Delta t < h$ confirming a first order accurate LTE. It could be erroneously deduced that the first order accuracy depends on the fact that the Taylor series (32) was truncated to $O(\Delta t^2)$ hence, another test has been performed along with the boundary conditions still deduced from (32), but while taking into account terms up to $O(\Delta t^3)$ and expressing $\partial_{tt}\mathbf{v}^*$ from Equation (21). As a result, no relevant modification in the error slope appears in Figure 7. Both curves have second order slopes still confirming the fact that the differential equation for $\mathbf{v}^*$ proposed in Reference [6] is not congruent to that required by the AB/CN scheme.

Finally, the computation was repeated but this time by adopting the AB/CN scheme associated to our proposal provided by Equation (33) and forward/backward discretization close to the boundary. Now, both curves in Figure 8 have third order slopes confirming the actual second order time accuracy of the pressure-free FTSM. The third order slope, definitively demonstrates that, the AB/CN scheme requires congruent boundary conditions otherwise, the updated tangential velocity component is affected by a first order LTE.

It is well known that the order of accuracy k of a fully discretized scheme is defined as the rate for which the LTE goes to zero according to $C\Delta t^k$ (C is a constant), while maintaining constant the ratio $\Delta t/h$. Hence, a conclusive series of computations have been performed at $\Delta t/h = 10^{-2}$. Four computational grids have been adopted, with $h = \pi/5, \pi/10, \pi/20, \pi/40$

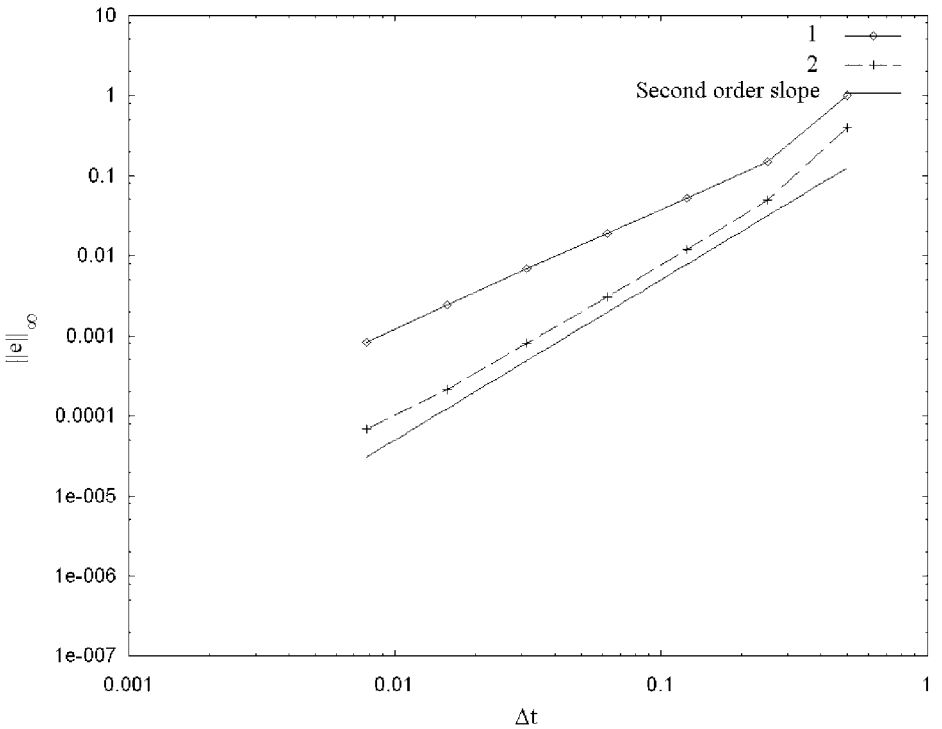

Figure 7. Analysis of the accuracy for the FTSM based on AB/CN time integration and second order FV discretization and Dirichlet boundary conditions based on expansion (32) truncated to $O(\Delta t^3)$. The errors, computed in the L_∞ norm in the domain Ω_1, are shown versus the time step in a double logarithmic scale for both u (curve 1) and v (curve 2) velocity components.

respectively, while the discretization error is now computed in the L_∞ norm at the final time of $\mathrm{T} = \pi/2$ and is reported in Figure 9, versus the grid size h in a double logarithmic scale. It is clear that the slope 2 is now monotone according to the fact that $\Delta t/h = const.$; of course, as the accuracy analysis is performed at $T = N\Delta t$ the second order slope is consistent with the $O(\Delta t^3)$ of the discretization error in a single step.

It was already observed that in the finite domain Ω_1 the solution $\mathbf{v}$ and the pressure gradient are (a priori) orthogonal in the sense of the inner product. Furthermore, the normal derivative of the pressure field along the boundaries vanishes and the numerical boundary layer does not entry into the velocity accuracy. In order to investigate the role of the normal pressure derivative, as well as of the location of the boundary, some computations with Dirichlet boundary conditions were performed also in the second finite domain $\Omega_2 = [0, \pi] \times [0, 1]$. Such a domain was chosen since the decomposition $(\mathbf{a}, \nabla p')$ is no longer a priori orthogonal (therein it results $\int_{\Omega_2} \mathbf{a} \cdot \nabla p' \, \mathrm{d}V = -0.510098\mathrm{e}^{-6t}$) while $\mathbf{n} \cdot \nabla p' \neq 0$ along the boundary $y = 1$ (see Figure 1(b)). It is interesting to compare now the numerical results for both domains.

To this goal, the CN time integration is now applied also in x-direction and the intermediate velocity is prescribed on all the frontier $\partial\Omega_2$. The two velocity components u^* and v^* assume the meaning of tangential or normal component depending on the considered axis. The tested

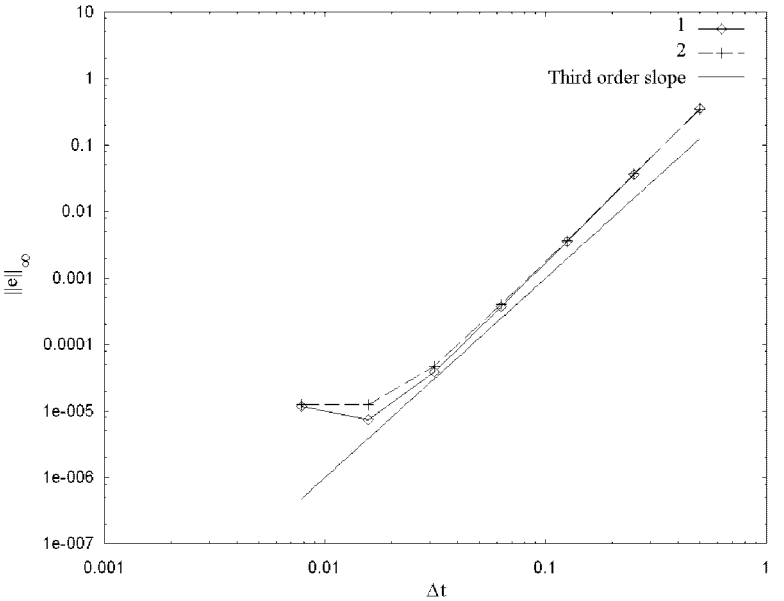

Figure 8. Analysis of the accuracy order for the FTSM based on AB/CN time integration and second order FV discretization and Dirichlet boundary conditions (34). The errors, computed in the L_∞ norm in the domain Ω_1, are shown versus the time step in a double logarithmic scale for both u (curve 1) and v (curve 2) velocity components.

expressions for computing $\mathbf{v}_\partial^{*n+1}$ are those according to these three different methods:

(a) simply assigned as the new velocity value, i.e., $\mathbf{v}_\partial^* = \mathbf{v}_\partial^{n+1}$ (analysed for example in References [6, 8, 11, 15, 17–21]) as such condition is still considered valid for accurate computations (see Reference [29]);
(b) the values are assigned according to the second order Taylor series (32) i.e. $\mathbf{v}_\partial^{*n+1} = \mathbf{v}_\partial^{n+1} + \Delta t \underline{\nabla} \langle \phi \rangle_\partial^n$ (see Reference [6]);
(c) Equation (33) is evaluated and assigned on the boundary;

The number of grid points is (315×101), i.e. one has the same computational grid size h of the previous computations, and the splitting error was again computed, after a single time step, in the L_∞ norm. The error evaluation includes the boundary points along which the tangential velocity component is effectively computed by means of $(31)_5$. The results are shown, for each one of the three cases, in the Figures 10(a)–10(d) concerning the errors on $u, v, \partial_x \langle \phi \rangle, \partial_y \langle \phi \rangle$, respectively. It clearly appears that the best accuracy is achieved by means of the present proposal. It is worthwhile remarking for case (a) that the first order slope of the velocity error curve indicates an $O(1)$ LTE, namely a non-consistent term.

Other computations were performed (not reported here) in these two different finite domains with a mixture of boundary conditions (b) and (c). These results confirmed that, when the decomposition is orthogonal, one could simply adopt anyone of normal condition (a) or (b) provided that the tangential condition is correctly derived from (c). In fact, the orthogonal projector allows us both to adjust the normal component and to recover fully second order accuracy into the interior. Conversely, when the decomposition is not orthogonal, this mixture

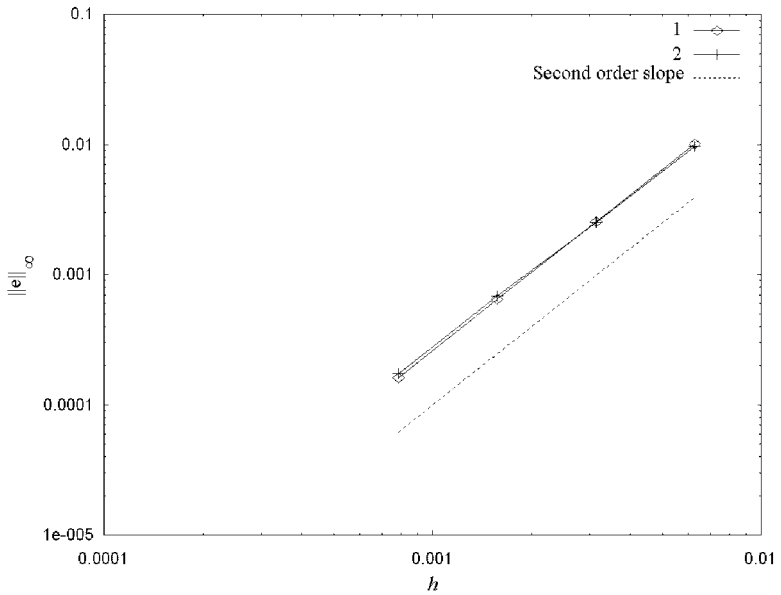

Figure 9. Analysis of the accuracy order for the FTSM based on AB/CN scheme and second order FV discretization and Dirichlet boundary conditions at a constant ratio $\Delta t/h = 10^{-2}$ (i.e. constant Courant number). The errors, computed in the L_∞ norm in the domain Ω_1 at time $T = \pi/2$, are now shown versus the grid sizes h in a double logarithmic scale for both u (curve 1) and v (curve 2) velocity components.

of boundary conditions results no longer applicable thus, in order to get a third order slope of the velocity error curves, is necessary to adopt condition (c) on the frontier for both velocity components.

As a final comment, it can be noticed that proposal (33) allows us to get a third order accurate tangential velocity in one time step but never the exact value. Nevertheless, after the projection step, the strategy to reset the tangential value to its correct one was tested in many performed simulations to produce a regular behaviour. It can be shown that by introducing $\partial_t \mathbf{v}^*$ expressed by Equation (7) into the third order Taylor series one gets $\mathbf{v}_\partial^{*n+1} = \mathbf{v}_\partial^{n+1} + \Delta t(I + (\Delta t/2)L_\mathrm{d})\underline{\nabla} p'|_\partial^n + (\Delta t^2/2)\partial_t \underline{\nabla} p'|_\partial^n + O(\Delta t^3)$. This expression can be considered the third order accurate counterpart of the condition proposed in [6] but, to be usefully discretized and computed on the boundary, it must be further manipulated. This other way to proceed is object of other study as expression (33) is fundamentally an explicit-based formulation and stability constraints, as well as the starting values construction (e.g. for impulsively starting flows) has to be *ad hoc* studied.

6. PERSPECTIVE STUDY IN THE ADOPTION OF THE PRESSURE-FREE FTSM INTO LARGE EDDY SIMULATION

A reliable behaviour of our proposal is that no approximation of the pressure gradient along the boundary is required and the expression (33) is simple to manage. Although the tangential

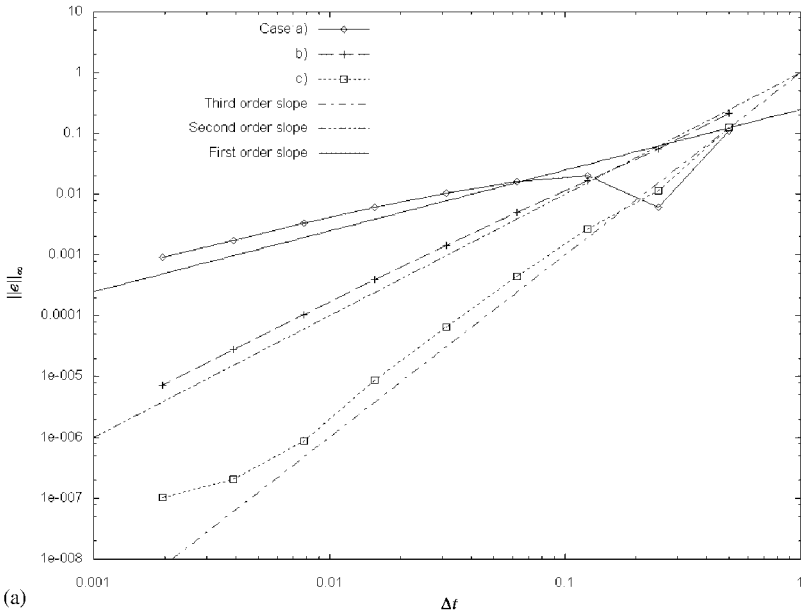

Figure 10. (a) Analysis of the accuracy order for the FTSM based on AB/CN time integration and second order FV discretization and Dirichlet boundary conditions prescribed on the whole boundary $\partial\Omega_2$ according to the cases (a)–(c). The errors, computed in the L_∞ norm, are shown versus the time step in a double logarithmic scale for the u velocity components. (b) The errors, computed in the L_∞ norm, are shown versus the time step in a double logarithmic scale for the v velocity components. (c) The errors, computed in the L_∞ norm, are shown versus the time step in a double logarithmic scale for the gradient component $\partial_x\langle\phi\rangle$. (d) The errors, computed in the L_∞ norm, are shown versus the time step in a double logarithmic scale for the gradient component $\partial_y\langle\phi\rangle$.

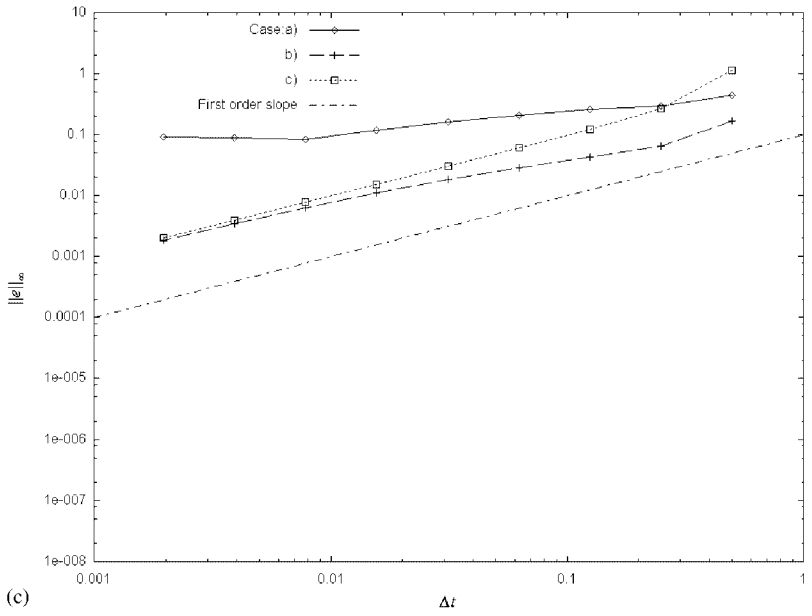

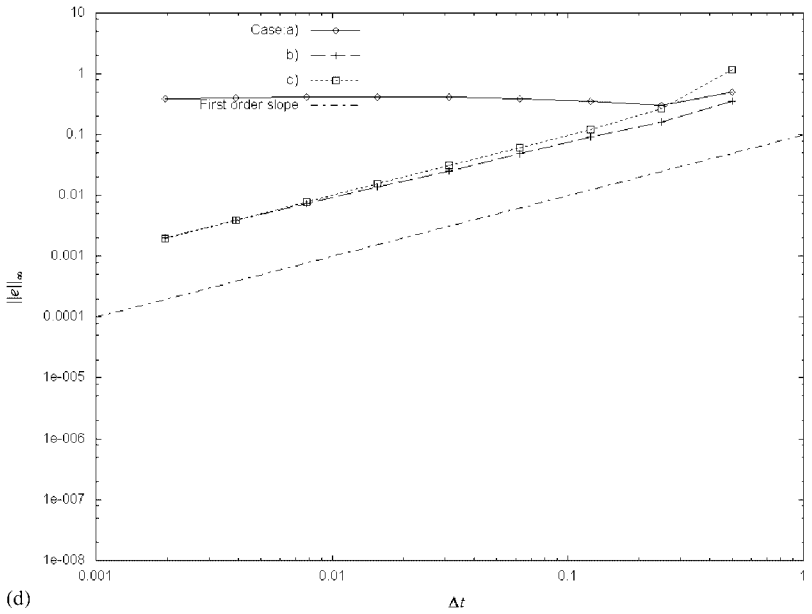

Figure 10. (*Continued*).

velocity component remains always approximated, it has now an $O(\Delta t^3)$ error. Hence, the strategy to reset, after each time step, the value to the correct one leads to a most likely regular behaviour, as we tested in many performed simulations.

In our knowledge, there are not published papers with studies on the main effects due to the coupling between the splitting methodology and the large eddy simulation (LES) equations modelling. Such an analysis is fundamental for our general purposes that consist in developing a high order formulation for LES of turbulent flows based on a fractional methodology. In a series of papers on the local average method [30–32], the role of the higher accuracy order of the resolved (filtered) variable, with respect to the unresolved part, was investigated. Furthermore, a proper de-convolution procedure was proposed which leads to define a new differential balance equation for the evolution of a higher order filtered variable, say $\tilde{\mathbf{v}}$ (the tilde indicates now a filtering). At present, a fourth order accurate spatial discretization within the pressure-free FTSM is currently in progress [33]. In the framework of the so-called implicit structural models [34], our evolution equation for $\tilde{\mathbf{v}}$ corresponds to solve the original top-hat filtered LES equations with a generalised scale-similarity model. It is generally assumed in LES that the filtering effect associated to the time step can be disregarded, provided that the Courant number is sufficiently small [34]. Often, the AB/CN integration and the boundary conditions (32) is used in LES for solving the filtered equations thus, it can be debatable that the issue of the fractional decoupling has not been sufficiently analysed in LES related publications. In the light of the present analysis, the first order error near to the boundary, for example in a channel flow simulation, has to be avoided because it can lead to dramatic effects in the model integration. In fact, the sub-grid scale (SGS) model is introduced in the filtered momentum equation and it accounts for an additional tensor term, say $\mathbf{T}$, according to (if filtering and derivatives do commute)

$$\frac{\partial \tilde{\mathbf{v}}}{\partial t} + \underline{\nabla} \cdot (\widetilde{\tilde{\mathbf{v}}\tilde{\mathbf{v}}}) + \underline{\nabla} \tilde{p}' = \underline{\nabla} \cdot (\nu \underline{\nabla} \tilde{\mathbf{v}}) + \underline{\nabla} \cdot (\widetilde{\tilde{\mathbf{v}}\tilde{\mathbf{v}}} - \widetilde{\mathbf{v}\mathbf{v}}) \equiv \underline{\nabla} \cdot (\nu \underline{\nabla} \tilde{\mathbf{v}}) + \underline{\nabla} \cdot \tilde{\mathbf{T}} \tag{40}$$

that, owing to the specific form of the SGS stress tensor (e.g. and eddy viscosity model), can be integrated within the CN scheme while the AB integration applies on the other terms. As an example of this splitting methodology, it follows that the filtered prediction equation writes as

$$\begin{aligned} \left[I - \frac{\Delta t}{2} \underline{\nabla} \cdot (\nu_{\mathrm{LES}} \underline{\nabla}) \right] \mathbf{v}^{*n+1} = & \left[I + \frac{\Delta t}{2} \underline{\nabla} \cdot (\nu_{\mathrm{LES}} \underline{\nabla}) \right] \tilde{\mathbf{v}}^n \\ & - \frac{\Delta t}{2} [3 \underline{\nabla} \cdot (\widetilde{\tilde{\mathbf{v}}^n \tilde{\mathbf{v}}^n}) - \underline{\nabla} \cdot (\widetilde{\tilde{\mathbf{v}}^{n-1} \tilde{\mathbf{v}}^{n-1}})], \quad \mathbf{x} \in \Omega \\ \mathbf{v}_{\partial}^{*n+1} = & f(\tilde{\mathbf{v}}), \quad \mathbf{x} \in \partial\Omega \end{aligned} \tag{41}$$

being ν_{LES} the total viscosity (that is a function of time to be considered in the Taylor expansion) and $\mathbf{v}^{*n} = \tilde{\mathbf{v}}^n$ fulfilling the incompressibility constraint; Equation (41) clarifies the meaning of $\mathbf{v}^{*n+1}$ that accounts for both filtering and SGS modelling. Thus, by particularizing (7), the differential equation for $\mathbf{v}^*$, consistent to LES equation (41), is expressed as

$$\frac{\partial \mathbf{v}^*}{\partial t} = - \underline{\nabla} \cdot (\widetilde{\tilde{\mathbf{v}}\tilde{\mathbf{v}}}) + \underline{\nabla} \cdot (\nu_{\mathrm{LES}} \underline{\nabla} \tilde{\mathbf{v}}^*) \tag{42}$$

and, accordingly, the congruent boundary condition for (41) has to be derived similarly to Equation (33); moreover, the actual pressure gradient is approximated by a relation that particularizes (16).

Conversely, if one adopt the AB integration also for the SGS term the entire FTSM must be analysed in a different way for deriving appropriate boundary conditions for $\mathbf{v}^*$. Owing to the consequent linear system, this appears the most opportune strategy, as well.

However, all these issues require future studies as they involve the simultaneously appearance of filtering and modelling contribution. In our opinion, the importance of an analysis of the lack in the accuracy of tangential velocity component, associated to the projection methods in LES for confined flow, has not been sufficiently highlighted. This analysis is currently under development and this paper introduces the next framework issues.

7. CONCLUSIONS

In this paper, the analysis of the *splitting error* for both the continuous and discrete *pressure-free* FTSM, along with a proposal for consistent intermediate boundary conditions, was presented. It was clearly shown that the *Local Truncation Error* can be estimated from the expressions of the splitting errors as they are related to each other by the time step. The analysis of the error was subdivided into that one which is inherent to the splitting methodology and in that one due the semi-implicit AB/CN scheme associated to intermediate boundary conditions. The error expressions were first derived in the physical space by means of a theoretical analysis and then confirmed in numerical experiments.

In fact, it was shown that the adoption of the AB/CN scheme allows us to really get a high accuracy order without requiring any numerical correction in the method. In particular, the analysis showed why the AB/CN scheme produces an $O(\Delta t^3)$ splitting error in one time step as a consequence of the consistent time discretization of the gauge equations. However, the pressure gradient is the only involved variable that is first order approximated. In this way, it was highlighted which one between the two proposed continuous equations $\partial_t \mathbf{v}^* = \mathbf{R}^*$ must be adopted for expressing the correct intermediate boundary conditions. In fact, it was shown that the semi-implicit AB/CN scheme, along with improper boundary conditions, dramatically affects the global accuracy of the FTSM. Therefore, after having demonstrated the proper consistent differential equation, an original proposal consisting in a congruent boundary condition expression is herein derived, fulfilling the goal of accomplishing the closure of the problem with fully accuracy. In our knowledge, this procedure is new in the literature and can be easily implemented for confined flows.

The numerical accuracy study was performed, for all cases, in the L_∞ of the splitting errors obtained with reference to the exact 2-D solution representing periodical vortex decay into the whole real space. Furthermore, while assigning Dirichlet boundary conditions two different finite domains were adopted; in particular, both cases of boundary locations having a vanishing and not vanishing normal component of the pressure gradient are considered (i.e. orthogonal and not decomposition). By summarizing the results of this study in terms of the LTE, the numerical accuracy analysis can be two-folds performed: either by taking constant the mesh size or the Courant number (CFL). In the first case, a description of a possible erroneous interpretation of the results discussed in Reference [8] is given. The accuracy of the method is formally defined by the LTE magnitude order that, multiplied by the time step, provides the actual slope of the discretization error curve. It is clearly shown why, by taking constant the mesh size, one verifies a third order slope only for certain time steps Δt, then a transition to monotonic first order slope is caused by the $O(\Delta t h^2)$ term in the splitting error

(i.e. a constant contribution of the spatial term in the LTE). This is the correct convergence error behaviour in the L_∞ norm that one expects as a result of the time-space discretized method. Conversely, by taking the CFL constant, the slope is monotonically third order for a second order spatial discretization. Many computations demonstrated that our proposal is efficient and accurate and the goal of adopting the *pressure-free* method based on AB/CN scheme with fully second order accuracy is reached.

Finally, a future research to retain global high accuracy in the application of LES methodology on Navier–Stokes system is addressed. In fact, the decoupling can alter the form of the splitting error and cause great problems in evaluating turbulence modelling. This is the guideline that can be proposed for the next studies.

APPENDIX A: GENERAL DERIVATION OF THE SPLITTING ERROR

For addressing this issue in general, consider the simple linear convection–diffusion–production equation for a scalar variable φ

$$\frac{\partial\varphi}{\partial t}=\underline{\nabla}\cdot(-\mathbf{v}\varphi+\Gamma\underline{\nabla}\varphi)+\mu(\varphi)=[\underline{\nabla}\cdot(-\mathbf{v}+\Gamma\underline{\nabla})+\mathrm{P}]\varphi\equiv\left(\underbrace{L_\mathrm{c}+L_\mathrm{d}}_{L}+\mathrm{P}\right)\varphi \tag{A1}$$

where Γ constant diffusivity coefficient, L and P suitable operators acting on φ if they are not dependent on time, one derives also:

$$\begin{aligned}
&\frac{\partial^2\varphi}{\partial t^2}=\frac{\partial}{\partial t}[(L+\mathrm{P})\varphi]=(L+\mathrm{P})\frac{\partial\varphi}{\partial t}=(L+\mathrm{P})[(L+\mathrm{P})\varphi]=(L+\mathrm{P})^2\varphi\\
&\qquad\vdots\\
&\frac{\partial^k\varphi}{\partial t^k}=(L+\mathrm{P})^k\varphi
\end{aligned} \tag{A2}$$

having adopted a symbolic power of operators. By exploiting a Taylor series about the time t^n and by introducing the definition of exponential series of an operator, one has the exact solution of (A1) expressed at time t^{n+1} according to [22]

$$\begin{aligned}
\varphi^{n+1}&=\varphi^n+\Delta t\left.\frac{\partial\varphi}{\partial t}\right|^n+\frac{\Delta t^2}{2}\left.\frac{\partial^2\varphi}{\partial t^2}\right|^n+\cdots=\varphi^n+\Delta t(L+\mathrm{P})\varphi^n+\frac{\Delta t^2}{2}(L+\mathrm{P})^2\varphi^n+\cdots\\
&=\left[I+\Delta t(L+\mathrm{P})+\frac{\Delta t^2}{2}(L+\mathrm{P})^2+\cdots\right]\varphi^n\\
&=\sum_{\mathrm{j}=0}^{\infty}\frac{\Delta t^j}{j!}(L+\mathrm{P})^j\varphi^n\equiv\mathrm{e}^{\Delta t(L+\mathrm{P})}\varphi^n
\end{aligned} \tag{A3}$$

wherein $e^{\Delta t(L+P)}$) is the *solution operator* for Equation (A1). As an example of the splitting methodology, one could first perform the calculation of the convective–diffusive terms and then that of the forcing one:

$$\varphi^* = \sum_{j=0}^{\infty} \frac{\Delta t^j}{j!} L^j \varphi^n \equiv e^{\Delta t L} \varphi^n$$

$$\varphi^{**} = \sum_{j=0}^{\infty} \frac{\Delta t^j}{j!} P^j \varphi^* \equiv e^{\Delta t P} \varphi^* = e^{\Delta t P}(e^{\Delta t L} \varphi^n) \tag{A4}$$

One defines the consequent *splitting error* as

$$\begin{aligned} e_s \equiv \varphi^{n+1} - \varphi^{**} &= (e^{\Delta t(L+P)} - e^{\Delta t P} e^{\Delta t L})\varphi^n = \left\{ \left[I + \Delta t(L+P) + \frac{\Delta t^2}{2}(L+P)^2 + \cdots \right] \right. \\ &\quad \left. - \left(I + \Delta t P + \frac{\Delta t^2}{2} P^2 + \cdots \right) \left(I + \Delta t L + \frac{\Delta t^2}{2} L^2 + \cdots \right) \right\} \varphi^n \\ &= \left\{ \left[I + \Delta t(L+P) + \frac{\Delta t^2}{2}(L^2 + LP + PL + P^2) \right] \right. \\ &\quad \left. - \left[I + \Delta t(L+P) + \frac{\Delta t^2}{2}(L^2 + 2PL + P^2) \right] \right\} \varphi^n + \cdots \\ &= \left[\frac{\Delta t^2}{2}(LP - PL) \right] \varphi^n + O(\Delta t^3) = \Delta t O(\mathrm{LTE}) \end{aligned} \tag{A5}$$

that vanishes if the operators L and P do commute (i.e. if P does not depend on $\mathbf{x}$) otherwise, one gets $e_s = \Delta t O(\mathrm{LTE})$ standing LTE for the *local truncation error* associated to the splitting, whose order of magnitude defines the accuracy of the method.

It is worthwhile remarking that the splitting error (A5) will have a second order convergence rate in a single time step which one can accumulate to an $O(\Delta t)$ after $N = T/\Delta t$ time steps to reach some fixed time T. The *Strang splitting* [35] is a particular modification of the fractional method that allows us to recover second order accuracy for operators with more general properties. The idea is to solve the first sub-problem over only a half time step then use the solution for a full time step on the second sub-problem; finally the third step is again performed over a half time step. For non-linear equations, the method remains second order accurate on smooth solutions [22] but, generalizations to systems of conservation laws (e.g. Navier–Stokes), must account for other constraints necessary to obtain a unique entropy-satisfying (weak) solution [36]. It means, for example, that the use of backward partial time-steps is constrained within thermodynamic postulates on to the non-negative entropy production. This analysis is out of the aims of the paper and the splitting errors that will be evaluated in the following sub-sections are those specific to the projection methods for NS equations for incompressible flows.

APPENDIX B: PROOF OF CONSISTENCY FOR THE INTERMEDIATE BOUNDARY CONDITION

The consistency of our proposal (34) can be reported into the framework of the analysis of the gauge equation, similarly to what performed in Section 4.1.2; now, one has to consider instead of Equation (7), the function $\mathbf{R}^* = L_c\mathbf{v} + (\partial_{xx}\mathbf{v} + \partial_{yy}\mathbf{v}^*)/Re \equiv (L_c + L_{dx})\mathbf{v} + L_{dy}\mathbf{v}^*$ (the diffusion operator was split along the two directions) and use its time derivative into the third order Taylor series, obtaining:

$$
\begin{aligned}
\mathbf{v}^{*n+1} &= \mathbf{v}^{*n} + \Delta t \left.\frac{\partial \mathbf{v}^*}{\partial t}\right|^n + \frac{\Delta t^2}{2} \left.\frac{\partial^2 \mathbf{v}^*}{\partial t^2}\right|^n + O(\Delta t^3) \\
&= \mathbf{v}^{*n} + \Delta t \mathbf{R}^*|^n + \frac{\Delta t^2}{2} \left.\frac{\partial \mathbf{R}^*}{\partial t}\right|^n + O(\Delta t^3) \\
&= \mathbf{v}^{*n} + \Delta t \mathbf{R}^*|^n + \frac{\Delta t^2}{2} \left.\left[\frac{\partial L_c}{\partial t}\mathbf{v} + (L_c + L_{dx})\frac{\partial \mathbf{v}}{\partial t} + L_{dy}\frac{\partial \mathbf{v}^*}{\partial t}\right]\right|^n + O(\Delta t^3) \\
&= \mathbf{v}^{*n} + \Delta t \mathbf{R}^*|^n + \frac{\Delta t^2}{2}\{-\nabla\cdot[(\mathbf{R}+\mathbf{P})\mathbf{v}] + (L_c + L_{dx})(\mathbf{R}+\mathbf{P}) + L_{dy}\mathbf{R}^*\}|^n + O(\Delta t^3) \\
&= \mathbf{v}^n + \Delta t \mathbf{R}^n + \frac{\Delta t^2}{2}\{-\nabla\cdot[(\mathbf{R}^n+\mathbf{P}^n)\mathbf{v}^n] + (L_c^n + L_{dx})\mathbf{P}^n + L^n\mathbf{R}^n\} + O(\Delta t^3) \\
&= \mathbf{v}^n + \Delta t \mathbf{R}^n + \frac{\Delta t^2}{2}\{-\nabla\cdot[(\mathbf{R}^n+\mathbf{P}^n)\mathbf{v}^n] + L^n(\mathbf{R}^n+\mathbf{P}^n) - L_{dy}\mathbf{P}^n\} + O(\Delta t^3)
\end{aligned}
\tag{A6}
$$

and compare the expression to that corresponding to our proposal (33)

$$
\begin{aligned}
\mathbf{v}^{*n+1} &= \left(I + \frac{\Delta t}{2}L_{dy} + \frac{\Delta t^2}{4}L_{dy}^{(2)}\right) \\
&\quad \times \left\{\left(I + \frac{\Delta t}{2}L_{dy}\right)\mathbf{v}^n + \frac{\Delta t}{2}[L_{dx}(3\mathbf{v}^n - \mathbf{v}^{n-1}) + 3L_c^n\mathbf{v}^n - L_c^{n-1}\mathbf{v}^{n-1}]\right\} \\
&= \left(I + \frac{\Delta t}{2}L_{dy}\right)^{(2)}\mathbf{v}^n + \frac{\Delta t^2}{4}L_{dy}^{(2)}\mathbf{v}^n + \left(\frac{\Delta t}{2} + \frac{\Delta t^2}{4}L_{dy}\right) \\
&\quad \times (3L_{dx}\mathbf{v}^n - L_{dx}\mathbf{v}^{n-1} + 3L_c^n\mathbf{v}^n - L_c^{n-1}\mathbf{v}^{n-1}) + O(\Delta t^3) \\
&= \left(I + \Delta t L_{dy} + \frac{\Delta t^2}{2}L_{dy}^{(2)}\right)\mathbf{v}^n + \left(\frac{\Delta t}{2} + \frac{\Delta t^2}{4}L_{dy}\right)[2(L_{dx} + L_c^n)\mathbf{v}^n \\
&\quad + \Delta t L_{dx}\left.\frac{\partial \mathbf{v}}{\partial t}\right|^n + \Delta t \left.\frac{\partial (L_c\mathbf{v})}{\partial t}\right|^n] + O(\Delta t^3)
\end{aligned}
$$

$$
\begin{aligned}
&= \left(I + \Delta t L_{\mathrm{d}y} + \frac{\Delta t^2}{2} L_{\mathrm{d}y}^{(2)}\right)\mathbf{v}^n + \Delta t(L_{\mathrm{d}x} + L_{\mathrm{c}}^n)\mathbf{v}^n \\
&\quad + \frac{\Delta t^2}{2}\left[L_{\mathrm{d}x}\left.\frac{\partial \mathbf{v}}{\partial t}\right|^n + \left.\frac{\partial L_{\mathrm{c}}\mathbf{v}}{\partial t}\right|^n + L_{\mathrm{d}y}(L_{\mathrm{d}x} + L_{\mathrm{c}}^n)\mathbf{v}^n\right] + O(\Delta t^3) \\
&= \mathbf{v}^n + \Delta t\mathbf{R}^n + \frac{\Delta t^2}{2}\{L_{\mathrm{d}y}^{(2)}\mathbf{v}^n + (L_{\mathrm{d}x} + L_{\mathrm{c}}^n)(\mathbf{R}^n + \mathbf{P}^n) - \underline{\nabla}\cdot[(\mathbf{R}^n + \mathbf{P}^n)\mathbf{v}^n] \\
&\quad + L_{\mathrm{d}y}(\mathbf{R}^n - L_{\mathrm{d}y}\mathbf{v}^n)\} + O(\Delta t^3) \\
&= \mathbf{v}^n + \Delta t\mathbf{R}^n + \frac{\Delta t^2}{2}\{(L_{\mathrm{d}x} + L_{\mathrm{c}}^n)(\mathbf{R}^n + \mathbf{P}^n) - \underline{\nabla}\cdot[(\mathbf{R}^n + \mathbf{P}^n)\mathbf{v}^n] + L_{\mathrm{d}y}\mathbf{R}^n\} + O(\Delta t^3) \\
&= \mathbf{v}^n + \Delta t\mathbf{R}^n + \frac{\Delta t^2}{2}\{L^n(\mathbf{R}^n + \mathbf{P}^n) - \underline{\nabla}\cdot[(\mathbf{R}^n + \mathbf{P}^n)\mathbf{v}^n] - L_{\mathrm{d}y}\mathbf{P}^n\} + O(\Delta t^3) \qquad \text{(A7)}
\end{aligned}
$$

demonstrating that (A7) and (A6) are exactly the same.

The consistency of (33) towards the projection problem (30) is shown by the fact that by taking the divergence one gets by definition the Poisson equation in $\langle\phi\rangle$ being:

$$
\nabla^2\langle\phi\rangle^{n+1} = \frac{1}{\Delta t}\underline{\nabla}\cdot\mathbf{v}^{*n+1} = \frac{1}{\Delta t}\underline{\nabla}\cdot\left(I + \frac{\Delta t}{2}L_{\mathrm{d}y} + \frac{\Delta t^2}{4}L_{\mathrm{d}y}^{(2)}\right)\mathbf{q}' \qquad \text{(A8)}
$$

associated to the boundary condition $\mathbf{n}\cdot\underline{\nabla}\langle\phi\rangle_{\partial}^{n+1} = \mathbf{n}\cdot(\mathbf{v}_{\partial}^{*n+1} - \mathbf{v}_{\partial}^{n+1})/\Delta t$ ensuring the existence and uniqueness of the solution. By simply integrating over Ω_k and applying the Gauss theorem, the exact integral form of Equation (30) is obtained.

REFERENCES

1. Ladyzhenskaja OA. *The Mathematical Theory of Viscous Incompressible Flow*. Gordon and Breach: New York, 1963.
2. Chorin AJ. Numerical solution of the Navier–Stokes equations. *Mathematics of Computing* 1968; **22**:745–762.
3. Temam T. Sur L'approximation de la Solution des Équations de Navier–Stokes par la Méthode de Pas Fractionnaires (II). *Archives of Rational Mechanics and Analysis* 1969; **33**:377–385.
4. Chorin AJ. On the convergence of discrete approximations to the Navier–Stokes equations. *Mathematics of Computing* 1969; **23**:341–353.
5. Chorin AJ, Marsden JE. *A Mathematical Introduction to Fluid Mechanics. Texts in Applied Mathematics*, vol. 4. Springer-Verlag: Berlin, 1990.
6. Kim J, Moin P. Application of a fractional-step method to incompressible Navier–Stokes equations. *Journal of Computational Physics* 1985; **59**:308–323.
7. Van Kan J. A second order accurate pressure correction scheme for three-dimensional incompressible flow. *SIAM Journal of Scientific Computing* 1986; **7**:870–891.
8. Perot JB. An analysis of the fractional step method. *Journal of Computational Physics* 1993; **108**:51–58.
9. Abdallah S. Comments on the fractional step method. *Journal of Computational Physics* 1995; **117**:179.
10. Perot JB. Comments on the fractional step method. *Journal of Computational Physics* 1995; **121**.
11. E W, Liu JG. Projection method I: convergence and numerical boundary layers. *SIAM Journal of Numerical Analysis* 1995; **32**(4):1017–1057.
12. E W, Liu JG. Projection method II: Godunov-Ryabenki analysis. *SIAM Journal of Numerical Analysis* 1996; **33**(4):1597–1621.
13. E W, Liu JG. Projection method with spatial discretization, available on blue http://www.math.princeton.edu/∼weinan/.
14. E W, Liu JG. Finite difference schemes for incompressible flows in the velocity–impulse formulation. *Journal of Computational Physics* 1997; **130**:67–76.

15. Shen J. On error estimates of the projection methods for the Navier–Stokes equations: second-order schemes. *Mathematics of Computing* 1996; **65**:1039–1065.
16. Guermond JL. Un Résultat de Convergence d'Ordre Deux En Temps Pour L'Approximation Des Équations De Navier–Stokes Par Une Technique De Projection Incrémentale. *Mathematical Modelling and Numerical Analysis* 1999; **33**(1):169–189.
17. Strikwerda JC, Lee YS. The accuracy of the fractional step method. *SIAM Journal of Numerical Analysis* 1999; **37**(1):37–47.
18. Wetton BR. Error analysis for Chorin's original projection method with regularization in space and time. *SIAM Journal of Numerical Analysis* 1997; **34**:1683–1697.
19. Wetton BR. Error analysis for pressure increment schemes, accepted in *SIAM Journal of Numerical Analysis*, January, 2000. Available at blue http://www.math.ubc.ca/∼wetton/.
20. Quarteroni A, Saleri F, Veneziani A. Factorisation methods for the numerical, approximation of Navier–Stokes equations. *Report EPFL/DMA 9.98*, *Computer Methods in Applied Mechanics and Engineering*, 1999. Available at blue http://dmawww.epfl.ch/Quarteroni-Chaire/publications.html.
21. Brown DL, Cortez R, Minion ML. Accurate projection methods for the incompressible Navier–Stokes equations. *Journal of Computational Physics* 2001; **168**.
22. Leveque RJ. *Finite Volume Methods for Hyperbolic Problems*. Cambridge: Cambridge Press, 2002.
23. Kantorovic LV, Akilov GP. *Analisi Funzionale*. Ed. MIR: Mosca, 1980.
24. Denaro FM. On the application of the Helmholtz-Hodge decomposition in projection methods for incompressible flows with general boundary conditions. *International Journal for Numerical Methods in Fluids* 2003, submitted.
25. Schiestel R, Viazzo S. A Hermitian-Fourier numerical method for solving the incompressible Navier–Stokes equations. *Computers & Fluids* 1995; **24**(6):739–752.
26. Almgren AS, Bell JB, Szymczak WG. A numerical method for the incompressible Navier–Stokes equations based on an approximate projection. *SIAM Journal of Scientific Computing* 1996; **17**:358–369.
27. LeVeque RJ. Intermediate boundary conditions for LOD, ADI and approximate factorization methods. *ICASE report no.85-21*, NASA Langley Research Center, Hampton, Virginia, 1985.
28. Gustafsson B. The convergence rate for difference approximation to mixed initial boundary value problems. *Mathematics of Computing* 1975; **29**:396–406.
29. Ye T, Mittal R, Udaykumar HS, Shyy W. An accurate cartesian grid method for viscous incompressible flows with complex immersed boundaries. *Journal of Computational Physics* 1999; **156**:209–240.
30. Denaro FM. Towards a new model-free simulation of high-Reynolds-flows: Local average direct numerical simulation. *International Journal for Numerical Methods in Fluids* 1996; **23**:125–142.
31. De Stefano G, Denaro FM, Riccardi G. Analysis of 3-D backward facing step incompressible flows via a local average-based numerical procedure. *International Journal for Numerical Methods in Fluids* 1998; **25**:797–835.
32. De Stefano G, Denaro FM, Riccardi G. High order filtering formulation for control volumes simulation of turbulent flows. *International Journal for Numerical Methods in Fluids* 2001; **37**(7).
33. Iannelli P, Denaro FM, De Stefano G. A deconvolution-based fourth order finite volume method for incompressible flows on non-uniform grids. *International Journal for Numerical Methods in Fluids*, 2002, submitted.
34. Sagaut P. *Large Eddy Simulation for Incompressible Flows. An Introduction*. (II edn). Springer: Berlin, 2002.
35. Strang G. On the construction and comparison of difference schemes. *SIAM Journal of Numerical Analysis* 1968; **5**:506–517.
36. Crandall MG, Majda A. The method of fractional steps for conservation laws. *Mathematics of Computing* 1980; **34**:285–314.

